Masters Program in Geospatial Technologies

# *Semi-Automated Workflow for Natural Disaster Assessment: A Case Study of Banda Aceh, Indonesia*

Abuzar Popal

Dissertation submitted in partial fulfilment of the requirements for the Degree of *Master of Science in Geospatial Technologies*

NOVA IMS · Universitat Jaume I

# Semi-Automated Workflow for Natural Disaster Assessment: A Case Study of Banda Aceh, Indonesia

Dissertation supervised by:

PhD Mario Caetano,

PhD Marco Painho,

PhD Ignacio Guerrero,

February 2016

# ACKNOWLEDGNEMENTS

I would like to thank my supervisors Mario Caetano, Marco Painho and Ignacio Guerrero for their continued feedback, support and guidance during the course of the dissertation.

I would also like to thank my family for their continued support and encouragement throughout the process.

# Semi-Automated Workflow for Natural Disaster Assessment: A Case Study of Banda Aceh, Indonesia

## ABSTRACT

The past decade has witnessed many natural disasters hitting highly populated areas causing billions of dollars in damage as well as many human casualties. During natural disasters, when attaining ground measurements are limited, remote sensing and geographical information systems (GIS) are useful tools for in-depth analysis of the affected area. This report will introduce a new semi-automatic workflow in which the road network will be used to break up the area into "blocks" and then zonal statistics will be applied to detect change based on the created blocks rather than the conventional methods of change detection; pixel by pixel and object oriented. This hybrid approach will take advantage of the simplicity and ease of applying pixel change detection methods on fixed objects or "blocks" to assess for damage. The change detection analysis results can then be used to map and quantify damage caused by natural disasters using pre and post Landsat imagery of the affected area. Multi-Criteria Analysis is performed on the damage map, proximity to roads, proximity to waterbodies and building size to find the most suitable locations for temporary housing sites.

The image differencing of NDWI mean produced the highest overall accuracy of 71.70% among eleven bands/indices and the multi-criteria analysis successfully selected fourteen temporary housing center sites from a possible 114. When time is of essence with limited resources and GIS expertise on the field, local authorities can greatly benefit from a rapid generalized analysis that will provide a "bird-eye view" of the affected area to efficiently and effectively allocate emergency efforts within a short time frame.

# KEYWORDS

Disaster Management

Damage Assessment

Natural Disaster Change Detection

Multi-Criteria Analysis

ArcGIS

FME

Python

# ACRONYMS

**LULC** – Landuse Landcover

**IDNDR** – International Decade for Natural Disaster Reduction

**GIS** – Geographic Information Systems

**TM** – Thematic Mapper

**NDVI** – Normalized Difference Vegetation Index

**NDBI** – Normalized Difference Build-up Index

**NDWI** – Normalized Difference Water Index

**MCA** – Multi-Criteria Analysis

**OSM** – Open Street Map

**DMSG** – Disaster Management Support Group

**WHO** – World Health Organization

**UN** – United Nations

**NIMS** – National Incident Management System

**MLC** – Maximum Likelihood Classifier

**PCA** – Principle Component Analysis

**SVM** – Support Vector Machine

**NN** – Nearest Neighbor

**MCDA** – Multi-Criteria Decision Analysis

**NIR** – Near Infrared

**ETM** – Thematic Mapper Plus

**MNDWI** – Modified Normalized Difference Water Index

**SAVI** – Soil Adjusted Vegetation Index

**FME** – Feature Manipulation Engine

## INDEX OF TEXT

# INDEX OF FIGURES

# INDEX OF TABLES

# 1 INTRODUCTION

## 1.1 Overview

The increase in readily available remote sensed data from satellites and aerial photography has developed into an essential tool for resource and disaster management as well as many other applications (Weih Jr 2010). Remote sensed data has increased the speed, precision and cost efficiency of forming spatial analysis for a particular purpose as well as development of spatial pattern maps that previously wasn't possible without ground truth samples (McRoberts 2007). With the increasing availability of satellite data, many large-scale specialized methods have been developed using change detection for forest cover change (Fraser R.H. 2005) and burned areas estimation (Gitas I.Z. 2004). Another area where remote sensing is prominently used is in mapping changes due to urbanization and urban sprawl (Xian 2005).

The traditional multispectral classification methods used for urban change produces reasonable results, mainly below 80%, because of the nature of the urban class being heterogeneous and causing spectral confusion. In order to improve the classification accuracy, many methods have been formed that incorporate different procedures to improve built-up area abstraction (Dehvari 2009). The built-up areas of Washington D.C. was extracted with 85% accuracy using unsupervised classification method on NDVI differencing of multi-date Landsat imagery (Masek 2000). Another approach that combined multiple techniques was applied by Xu (2002), who used a supervised classification with mixture of signature analysis to select built-up areas in Fuqing City, China. The author improved the overall accuracy by incorporating the classification layer with the difference in spectral response between urban and non-urban classes. Xian (2005) produced accuracy of over 85% by combining an unsupervised classification with regression tree algorithm classification of build-up areas to measure the extension of built-up areas into watersheds in Florida.

In the past, Landuse/Landcover (LULC) mapping predominantly used pixel-based analysis to detect change. The change detection was executed by either using supervised classification, unsupervised classification or an amalgamation of both (Enderle 2005). Pixel-based analysis only compares the spectral properties of a pixel disregarding the spatial and environmental information of the pixel or group of pixels. The spatial information of the pixel can help generate more accurate approximations of LULC classifications (De Jong 2001). The rapid progress of satellites delivering high resolution imagery has developed new more effective methods in change detection analysis which using the traditional pixel-based methods creates

a “salt and pepper” effect that adds to the imprecision regarding the overall classification accuracy (Campagnolo 2007).

The possibility of creating a fully automated classification methods that would be an improvement over the pixel-based techniques that has been looked at for years (Blaschke 2000). Various computer software packages are created to analyze the characteristics of a pixel in a more object oriented manner which takes both the spectral and spatial properties. Feature Analyst and eCognition are two of the most widely used software packages that perform object-based classification in which a segmentation procedure coupled with iterative learning algorithms are applied to form a semi-automated classification process that has proven to be more accurate when comparing with pixel-based techniques especially with the availability of high resolution imagery (Blundell 2006).

The past decade has witnessed many natural disasters hitting highly populated areas causing billions of dollars in damage, socio-economic losses as well as many human casualties even with the International Decade for Natural Disaster Reduction (IDNDR) initiative in practice (Yamazaki 2001). Remote Sensing and Geographical Information Systems (GIS) are useful tools for in-depth analysis of an area affected by an unexpected natural disaster where attaining ground measurements are limited (Carrara 1999). GIS tools has been used for susceptibility assessment of areas affected by natural disasters (Yamazaki 2001). Over the years, many different analysis techniques have been developed to aid in geographical examination of the affected area which will then eventually support decision making (Cutter 2003). One remote sensing technique widely used for natural disaster assessment is change detection which identifies the differences in the state of an object over time using a pre and post-event imagery. Although the land and needs assessment is done within five days, more in-depth analysis regarding land loss, damage, availability and risk assessment can take up to six weeks (Fitzpatrick 2010). The short period after a disaster occurring is most crucial for humanitarian and aid relief efforts therefore a more generalized overview analysis is required taking everything regarding the response stage of the disaster cycle into consideration. The rapid increase in using geospatial derived data for decision support by policy makers is mainly due to its ability to continuously address operational requirements in an efficient and effective manner across all scales. The data forms the foundation for various in-depth natural disaster analysis such as risk assessment, mitigation planning, disaster assessment and response design (Tralli 2005). Rapid damage mapping is vital for visualizing areas affected by a natural disaster to adequately design and allocate disaster response and relief efforts. The use of imagery from both civil and commercial satellite providers such as IKONOS and SPOT are enduring increasing influence in disaster management processes (Tralli 2005).

It’s important to note, in spite of advancements in satellite imagery provisions raw satellite imagery is essentially unusable for non-expert users such as emergency relief workers or decision makers. For the created products to be fully understood by non-experts, damage maps, reports and statistics have to be obtained from processing, analysis and interpretation of the raw data by a GIS expert. One of the most important, frequently overlooked aspect of data processing and delivery is the direct interaction with the emergency assessment team and decision makers. Without a proper and concise explanation of the sophisticated image analysis, mapping and GIS products there is little meaningfulness derived from the products for the emergency response team. It’s as important to produce easily understandable products or to provide close contact concerning image analysis in order for non-GIS users such as decision makers to maximize the intake of the intended information of the products to make the appropriate decisions (Voigt 2007).

This report will introduce a new semi-automatic workflow in which the road network will be used to break up the area into “blocks” and then zonal statistics will be applied to detect change based on the created blocks rather than a pixel by pixel or object oriented method. This hybrid approach will take advantage of the simplicity and ease of applying pixel change detection methods on fixed objects or “blocks” to assess for damage. The change detection analysis results can then be used to map and quantify damage caused by natural disasters using pre and post Landsat imagery of the affected area. With the addition of auxiliary OSM data, more specific spatial analysis can be done for emergency response purposes such as locations of temporary housing sites during a disaster. When time is of essence with limited resources and GIS expertise on the field, local authorities can greatly benefit from a rapid generalized analysis that will provide a “bird-eye view” of the affected area to efficiently and effectively allocate emergency efforts within a short time frame.

## 1.2 Objectives

The objective of this research is to develop a semi-automated workflow to assess and quantify natural disaster damage. The accuracy results of two of the most commonly used pixel-change detection (ratio and differencing) methods will be compared based on artificially derived city “blocks” created by the road network. Change detection will be applied on six bands (excluding thermal band) of pre and post event Landsat 5 thematic mapper (TM) imagery as well specialized indices such as Normalized Difference Vegetation Index (NDVI), Normalized Difference Build-up Index (NDBI) and Normalized Difference Water Index (NDWI) to

evaluate which one produces the most accurate map. To further add supplementary value to the disaster damage map for emergency response purposes, using multi-criteria analysis (MCA) with the addition of auxiliary data (Open Street Map (OSM) data), the most suitable temporary housing sites will be selected to accommodate displaced individuals during a disaster.

# 2 THEORETICAL FRAMEWORK

## 2.1 Remote Sensing for Disaster Management

The advancement of remote sensing satellite systems and image-analysis methods in recent times have made earth-observation systems an integral part of emergency management for natural and humanitarian crisis situations (G. Bitelli 2001). The rapid improvements in coverage, spatial and temporal resolution of satellite imagery have attributed to this, as such:

a) Spatial resolution or pixel spacing has improved to a few meters precision for optical and radar data.

b) International satellite-based disaster-response possibilities have enhanced due to the rapid increase in communication, interoperability and networking between different satellite organizations as well as the increase in data derived from satellites.

c) Increase in number of international disaster research agencies such as Disaster Management Support Group (DMSG) and International Charter Space and Major Disasters (Eguchi 2001).

The plain observation and monitoring of present and future natural disasters was one of the main tasks of this international initiative, with the overall intention of enhancing the emergency management process. The various international disaster monitoring agencies combined are referred to as International Charter (Charter 2000). On a yearly basis, natural disasters are responsible for billions of dollars in property and economic damage as well as casualties numbering in the thousands. A study by the World Health Organization (WHO) showed that the nineteen years between 1964 and 1983 approximately 2.5 million people died from natural disaster events as well as displacing an additional 750 million. Due to the increasing concentration of people living in urban and coastal areas highly susceptible to the dangers of natural disaster events, initiatives had to be taken to reduce the impact of natural hazards (Voigt 2007). With the rapid advancement of both scientific and technological research and the availability of almost instantaneous satellite data, this provided unique opportunities to mitigate the impacts of natural disasters. The United Nations (UN) passed a resolution (1987) declaring the 1990's as the International Decade for Natural Disaster Reduction (IDNDR). The main goal

of the resolution was for 'the international community to pay special attention to fostering cooperation in the field of natural disaster reduction'. The UN resolution put forward the development of internationally cooperated strategies to decrease loss caused from natural disasters by focusing on different aspects of disaster management such as prevention and preparedness plus improving efforts designated to disaster relief, response and recovery (NDR 1991).

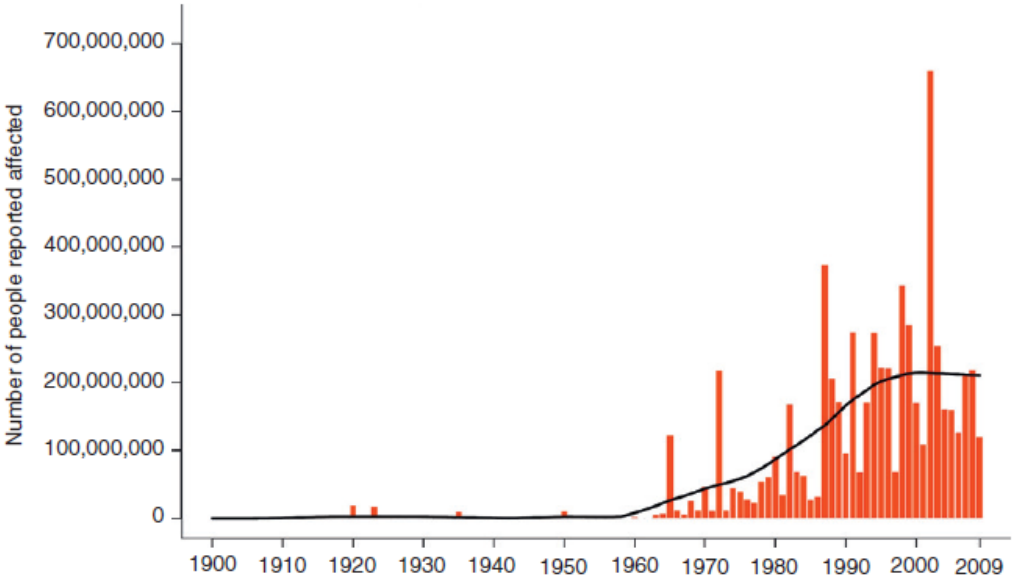


*Figure 1- Number of People Affected by Natural Disaster (UNDP 2004)*

As of the year 2000, it was estimated that at least 75% of the world's population lived in areas at risk from a major disaster (UNDP 2004). And because these high-risk areas periodically experience major disasters, it is a logical connection to say that the number of people who are annually affected by disasters is equally high ((ISDR) 2004)(Figure 1). The number of people moving from rural areas to cities also known as urbanization has increased dramatically over the years. In 1950, around 2.5 billion people lived in cities which accounts for less than 30% of the population compared to 5.7 billion people in 1998 that live in cities, which increased to 45% of the total population. The trend is set to continue according to UN estimates of 2025 which indicates 8.3 billion people will be living in cities, accumulating to 60% of the total population (Economic 2001). The current trend of natural disaster shows that the number of disaster occurrence is rising every year even though there are less human causalities from disaster events, more people are being affected. The reconstruction cost of disaster have become more expensive, with poorer countries experiencing far more economic consequences in the long term than wealthier nations largely due to the fact that rich countries have extra funds to absorb the cost whereas poorer countries reallocate money that was in place for development to absorb the cost, therefore hindering development.

### *2.1.1 Four Phases of Emergency Management*

The occurrence of a natural disasters such as floods, hurricanes, volcanoes, earthquakes, wildfires and other natural hazardous incidents are inevitable. Even though these events have great impacts and can cause catastrophic change within the natural environment, the occurrences are inherently part of the natural system. Natural environments have shown to have incredible resilience when it comes to damage from these events and have shown to regenerate and even restore habitat and ecosystems within a relatively short time period. When man-made environments are hit by these events, that's when the term "disaster" is used. The term "disaster" is used when man-made environments influencing human activity such as infrastructure, agricultural fields and other land uses crosses paths with natural forces. The human built environment is not as resilient as the natural one and an entire man-made community can be depleted and require many years to re-establish (Cutter 2003).

Although the effects of natural disasters cannot be completely ceased, reduction steps can be taken to mitigate the impact and the subsequent consequences. The advancement of modelling tools and methods that incorporate many different data sources in a timely manner will help avoid worse-case scenarios. By analysing current human activities and forecasting the future trends before a disaster occurs, the magnitude of the damage caused by the disaster can be greatly reduced by alleviating the negative effects. The need of creating a standard guide to decrease the susceptibility of people and infrastructure in affected areas was required to help decision makers, leaders and international aid groups in all stages of disaster management (USAID/OAS 1997). Four main elements of emergency management was formed to help governments deal with and create effective plans to mitigate the impacts of natural disasters by lessening hazard impact, prepare populations for the possibility of a hazard occurring, response measures if disaster has occurred, and assist with recovery actions to the affected nations and people for the coming months and years following a disaster (Keller 1996). The emergency management cycle is a multipart process that involves all phases of the natural disaster cycle from pre planning to recovery (Figure 2). The four components of an emergency management system are:


*Figure 2 – Four Components of Emergency Management (Safety 2010)*

• Mitigation actions are designed to reduce the physical and social damages caused from disaster events and therefore intersects all the phases of emergency management. The objective of this phase is to reduce human casualties and property damage by creating safer communities. This is achieved by risk analysis of the community to enforce specific building codes (constructing disaster-resistant structures), zoning requirements (subdivision regulations to discourage development in high-risk areas) and building artificial barriers such as levees. Education programs aimed to train the public regarding vital emergency procedures and how to protect their property against the forces of nature (USAID/OAS 1997).

• Preparedness actions increase the capability of a community in dealing with a disaster event. Preparedness is defined as, 'a continuous cycle of planning, organizing, training, equipping, exercising, evaluating, and taking corrective action in an effort to ensure effective coordination during incident response,' by The National Incident Management System (NIMS). Preparedness actions can be broadly divided into two groups, one being structural actions that deal with preparing for the immediate arrival of disaster, for example sandbagging coastal areas and the other being non-structural actions which helps reduce human casualties and property damage. Preparedness stage also deals with the design of the warning systems, improvement of response measures as well as preparing emergency methods and training emergency staff (Lindsay 2012).

• Response actions deals with efficient coordination of resources during or directly after a disaster where time is of essence. The response phase is intended to provide immediate help to the victims in practices such as medical care, food distribution, search and rescue operations and temporary shelter housing. This phase also includes a quick assessment of the affected area in terms of property damage, security and most importantly the victims in danger (Safety 2010).

• Recovery actions help the affected community get back to normal conditions and begins after the disaster has occurred. The emergency management activities include repair of basic services such as restoration of roads, power, water and other essential social, physical and economic damages that are vital for a community to function. In essence, recovery activities are aimed to reduce the effects of insecurity, lack of shelter, disaster, starvation and increasing number of victims (County n.d.).

### *2.1.2 Rapid Mapping*

The International Charter on Space and Major Disaster was created in 1999 to encourage international cooperation in terms of civil protection, emergency aid and security during a disaster by utilizing data from governmental satellites and national space agencies. From 1999 to 2006, the International Charter has been triggered over 100 times (Charter 2000) providing valuable information within a short time frame in terms of mapping and analysis products for emergency management. Seven major national space agencies are part of this initiative that make available the data acquired from their satellites once a disaster has occurred, these agencies are: NOAA (USA), ISRO (India), CONAE (Argentina), JAXA (Japan), CNES (France), ESA (Europe) and CSA (Canada). The agency shares a variety of data mostly in optical and radar platforms which include IRS, SAC-C, SPOT, MERIS, ERS, ENVISAT and RADARSAT (CEOS 2002).

The dissemination of fast up-to-date accurate image analysis products during the response and recovery phase of the emergency management cycle is the main focus of the International Charter. In addition, its purpose is to assist with disaster assessment especially in remote areas where attaining ground or other means of data is insufficient. Due to recent efforts of the International Charter, the access, delivery and access of satellite data can be implemented within a short time period (from hours to several days) which allows appropriate, timely and beneficial emergency response in the impact area. The International Charter offers a global mechanism to incorporate data from multiple satellites/agencies within a short timeframe and doesn't impede usual procedures. Therefore providing valuable disaster assessment information in a short time for on field non-expert users such as emergency relief works in addition to non-expert users dealing with policy/decision making and funding agencies. The readily up-to-date imagery provides the vital foundation for rapid analysis of location, situation, extent and population affected for a disaster event (Charter 2000, Allenbach 2005).

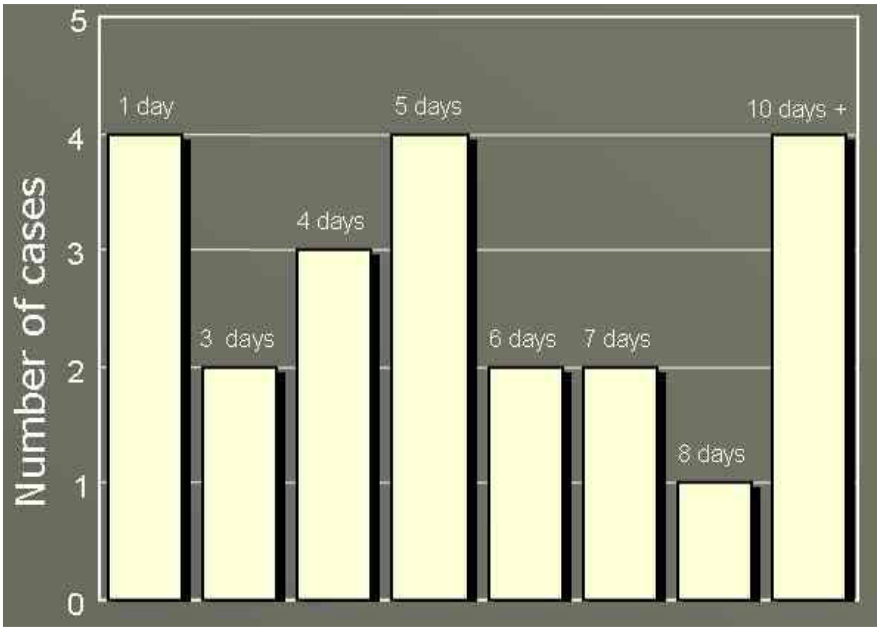


*Figure 3 – Number of Days Taken To Produce First Crisis Map (Allenbach 2005)*

During a disaster, the emergency management officials require information regarding the material and human impact as well as the location and the extent of the area affected to enable emergency response. In order to create precise reliable geographical content such as rapid mapping products the utilization and acquisition of Earth Observation (EO) information has to be done swiftly. One agency that provides rapid mapping services is SERTIT (Louis Pasteur University, Strasbourg, France) which works together with the French Space Agency (CNES) and European Space Agency (ESA) to furnish feedback on mapping products. The aim of SERTIT products are to provide valuable geographic information from satellite imagery. EO satellites provide both low and high resolution data that are utilized based on the mapping objective (CEOS 2002). In order for the raw data from multiple sources to be utilized, the data has to be formatted and go through a multi-process that requires the digital data obtained from the satellites to be manipulated and interpreted by remote sensing specialists while also being validated through computer assisted means. The transformation from raw data to geographic data has to done in a short time, since in rapid mapping production time is essential; the production cycle spans hours to days rather than a typical mapping cycle that requires weeks to months. The rapid mapping mission is to produce geographic mapping of areas affected by natural disasters within 12 hours of raw data acquisition by diffusion of all available sensors. Although the focus of the SERTIT is to decrease the time it takes to produce crisis maps, Figure 3 shows that in most cases it takes over 3 days from the time the event happens to the first crisis map. The figure is based on four years span of the Charters actions and with an average of 5 days with some events taking over 10 days, indicating there is much room for improvement in providing rapid crisis maps. The rapid mapping product consists of geo-referenced digital map

that incorporates newly created on-the-fly event map with reference satellite data. Due to its success in providing rapid mapping solutions for floods, this method was further adopted to provide rapid mapping for natural disasters as part of The International Charter on Space and Major Disaster's on-call operation service (Allenbach 2005).

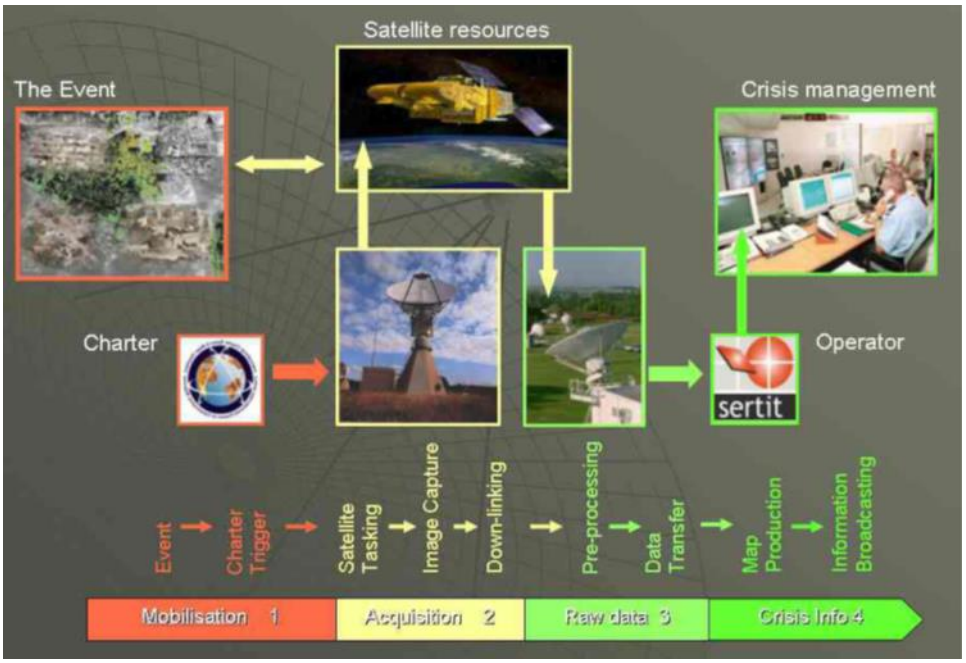


*Figure 4 – Flowchart of Crisis Mapping (Allenbach 2005)*

Once the Charter is triggered, it goes through four steps until a meaningful map is produced (Figure 4). The first step is mobilisation, its right after the disaster event when the charter is triggered followed by the acquisition step in which the image for the affected area is retrieved, then the pre-processing of the raw data and finally the informative map production. The International Charters products have been very beneficial to the disaster management domain but with increasing rate of disasters, (Voigt 2007) highlighted three areas in which further improvement is required. Firstly, the main product of this initiative is providing raw satellite imagery of the affected area rather than spatial analysis maps (ex. Damage assessment) which should be improved to foster quicker decision making in regards to natural disasters. Secondly, in order to improve migration efforts, the speed of information transfer has to be improved to maximize effective responsiveness. Thirdly, the cooperation, coordination and sharing mechanism between the existing partners need to improve with the aim to more efficiently deal with organizational, technical and data sharing (Charter 2000, Allenbach 2005).

There is a major challenge in the combination of local and global GPS data as well as combination between new and older datasets due to the absence of format standards

(GeoHazards 2004). Some examples of change detection analysis done from multiple sources are:

- Remote Sensing data can be utilized for assessing areas prone to earthquake activity as it provides up to date spatially continuous data on the tectonic landscape which can be used to better understand local fault systems. Using the capabilities of remote sensed data fused with ground data can provide better approximation of displacements and regional slip models of tectonic tension levels (Z. Cakir 2003).
- Combination of demographic data with a building infrastructure dataset and imagery to assess vulnerability and create post-disaster damage assessment for an area stricken by an earthquake (Rejaie 2004).
- To greatly reduce spectral confusion between urban and non-urban classes, Zhang (2002) performed post-classification change detection of Beijing, China by combining road density with information obtained from spectral bands which improved overall accuracy. Based on the road density, urban areas were distinguished from non-urban areas which provided a better platform for classification to occur on.
- Using band 4 and band 5 of the Landsat thematic mapper image, Zha (2003) developed the normalized difference built-up index (NDBI) to select urban areas in Najing City of China. The NDBI was customized to select urban areas which was combined with the NDVI image to remove vegetation noise within urban areas.

### *2.1.3 Automated Workflows for Mapping*

The continued advancement of remote sensing procedures to detect damage from satellite imagery has led to many approaches to automate the process. Hasegawa (2000) developed an automated approach to detect building damage from the Kobe (Japan) earthquake that only required post-event images. This automated method calculated damage comparatively well when compared to the reference data by undertaking edge detection using the multi-level slice technique combined with using threshold values of color indices. Using the same automated technique, damage detection for the 1999 Kocaeli (Turkey) earthquake produced moderate accuracy (H. Y. Mitomi 2000). Mitomi (2001) created an automated approach in which maximum likelihood classifier (MLC) was used to detect building damage in order to improve the overall accuracy. Another automated method similar to the previous example was produced to detect damage using high resolution aerial imagery after the Gujarat (India) earthquake. Although all these approaches show promising advancement in terms of damage assessment automation, many of the parameters of the automation are optimized to each image or geographic location. Due to the difference in image properties such as influence of the sun

(radiance and angle) and built environment, the automated image properties should be adjusted according to each image. Most automated methods are customized to a certain area of interest with multiple sources of data especially imagery at very high resolution. Although the automation can speed up the process of disaster assessment and map creation, the reliance on various data sources and its integration can hinder the overall process to consequential effects in terms of rapid mapping (Yamazaki 2001).

### *2.1.4 Specialized Indices*

Specialized indices are commonly used to enhance the sensitivity of a certain LULC feature by making use of the reflectance and absorption measures of the feature from the sun's radiation across a range of the electromagnetic spectrum. Surface features reflect and absorb sun's radiation differently across specific wavelengths of light. Specialized indices are created by the manipulation of the reflectance and absorption of a feature in different bands (wavelengths) and the following indices are used in this study:

- Normalized Difference Vegetation Index (NDVI),

Normalized difference vegetation index (NDVI) images are created to enhance the presence of vegetation (greenness) in an image. The index takes advantage of green vegetation having low reflectance in the red band range of a Landsat image and high reflectance in the near infrared range of the spectrum. The NDVI values range from 1 to -1, with green vegetation having positive values usually between 0.3 to 0.8, with soils having values within the range of 0.1 to 0.2 and clear water having values around 0. The development of the index has led to many possibilities into detecting vegetation change and has been widely used for crop assessment and deforestation applications (Jackson 1991). The Formula for obtaining the NDVI is as follows:

$$\mathrm{NDVI}_{i,c} = \frac{x_{i,\mathrm{NIR}} - x_{i,\mathrm{RED}}}{x_{i,\mathrm{NIR}} + x_{i,\mathrm{RED}}}$$

where the influence of NIR is maximized and red band minimized in order to enhance the vegetated green areas of the image. Even though NDVI is not a fundamental physical quantity of vegetation, it is highly correlated with physical properties of vegetation cover such as leaf area index, fractional vegetation cover, biomass and vegetation condition which makes it a beneficial measurement regardless of its limitation (Jackson 1991).

- Normalized Difference Built-up Index (NDBI),

In order to enhance the properties of built-up areas in an image, Zhang (2003) developed the normalized difference build-up index (NDBI) with the following equation:

$$\mathrm{NDBI}_{i,c} = \frac{x_{i,\mathrm{MIR}} - x_{i,\mathrm{NIR}}}{x_{i,\mathrm{MIR}} + x_{i,\mathrm{NIR}}}$$

The NDBI is developed by subtracting the shortwave infrared (MIR) by the near infrared band and dividing by MIR plus NIR, in order to improve the spectral reaction of built-up. This is effective due to the fact that built-up areas have higher reflectance in the MIR wavelengths than the NIR (Gao 1996). Even though NDBI images produce positive values for built-up areas, it often confuses with vegetated areas that also have positive values. Xu's (2006) research found that both vegetation and turbid waters also reflect MIR more than NIR which added unwanted noise.

- Normalized Difference Water Index (NDWI).

With the use of multi-band imagery, there are two district ways of extracting water features. One method is through analysis of signature values of water against other features using different spectral bands and then applying a logical statement to distinguish water from land (H.-q. Xu 2002). The other more frequently used method is by applying a band-ratio in order to enhance the water features while subduing the effects of vegetation and land features (H. Xu 2006). This was developed through the use of the bands corresponding to the green and near infrared (NIR) wavelengths and the formula is stated as follows (McFeeters 1996):

$$NDWI = \frac{Green - NIR}{Green + NIR}$$

The normalized difference water index (NDWI) consist of band 2 (green) and band 4 (NIR) of the thematic mapper. The NDWI index subtracts the green band by the NIR band, the result is divided by the green band plus the NIR band in order to enhance the presence of water. The index maximizes the high reflectance of water in the green band whereas minimizing the low reflectance of water in the NIR band, which has high reflectance of vegetation and soil features (H. Xu 2006). The outcome of the index is having positive values for water and zero or negative numbers for vegetation and soil features (McFeeters 1996).

Using Landsat thematic mapper (TM) and enhanced thematic mapper plus (ETM) imagery Xu (2007) used three indices, normal difference built-up index (NDBI), modified normalized difference water index (MNDWI) and soil adjusted vegetation index (SAVI) to extract urban built-up land features. The method used supervised classification, principal components

analysis as well as a logic calculation to extract urban built-up areas with an overall accuracy ranging from 91.5% to 98.5%. The use of indices in a composite image rather than the original seven-band images increased the distinguishability of the spectral signatures between the classes.

## 2.2 Change Detection Overview

Singh (1989) defined change detection as, 'the process of identifying differences in the state of an object or phenomenon by observing it at different times'. The process of identifying differences in change detection can be applied at different scales over time periods, with refined spectral and spatial resolutions from a comprehensive section of the electromagnetic spectrum. To have a positive influence on disaster management processes, the data gathered and integrated from various sources have to meet the required accuracy, spatial scope and be utilized within the required timeframe (Tralli 2005).

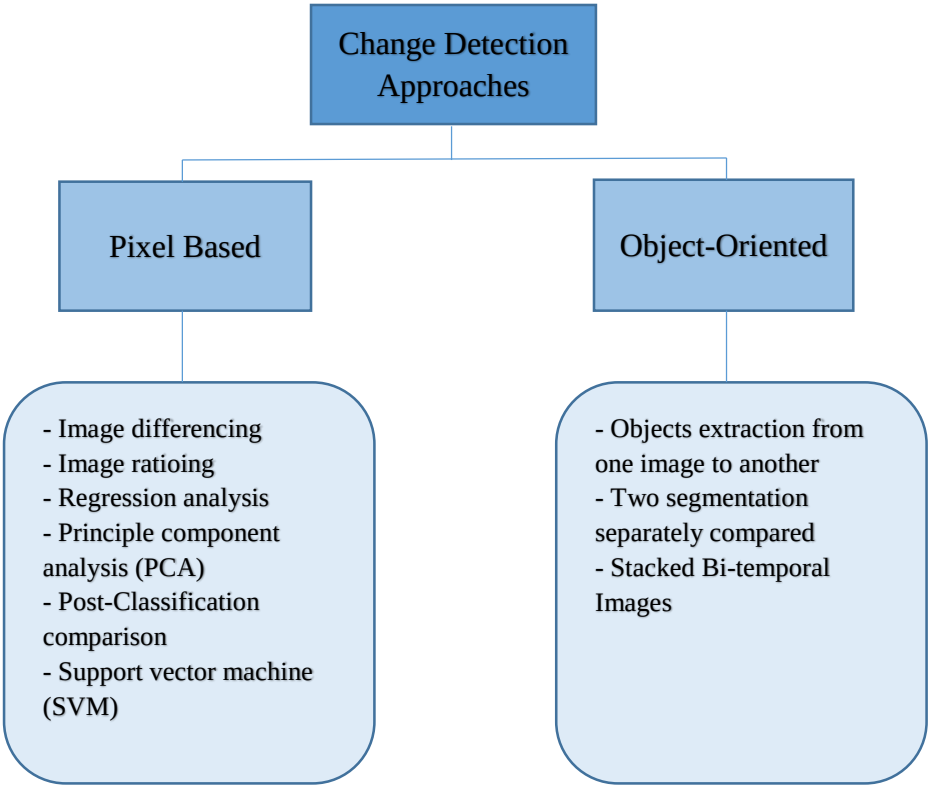


*Figure 5 – Change Detection Approaches*

There are two main approaches to remote sensing change detection: Pixel-based and Object-oriented. Pixel-based performs change detection on only the spectral properties of corresponding pixels from imagery of the same area at different times whereas object-oriented takes into consideration the surrounding environment of the pixel as well. Figure 5 shows the main techniques used for both approaches, although there was been great advances in object-oriented techniques, the most widely used methods are image differencing and ratioing due to

its simplicity. Image differencing is applied by subtraction of images pixel by pixel and band by band between images taken in different times. Image Ratioing is also a simple mathematical calculation but instead of subtraction, it's the ratio between the images. The simplicity of the calculation results can be seen in Figure 6, where in the differencing method no change is indicated by 0 (subtracting same pixel value) and the ratio method producing a value of 1 (dividing by same pixel value). The outcome of a pixel-based classification are square pixels while object-oriented classification produces a more realistic result that creates entities of various shapes and size. This is known as multi-resolution segmentation in which pixels are grouped into uniform image objects that occur in different sizes concurrently. Since the objects are classified based on spatial context, geometry and texture rather than just a single pixel, the object-oriented segmentation follow natural landscapes more realistically. Multiple bands with various resolutions of different formats can be incorporated in order to better execute an object-based classification. Data in different forms such as infrared, shapefiles and elevations can be coupled into an object-based image analysis simultaneously. Supervised classification is similar to the nearest neighbor (NN) classification used in object-oriented analysis that takes into consideration the vicinity relations, nearness and distance between the multiple layers which conveys context to the analysis. After the segmentation, the user provides the training data for the landcover classes on which the image object statistics are based on. Once the statistics have been defined for each landcover type, the objects are classified accordingly (Dehvari 2009).

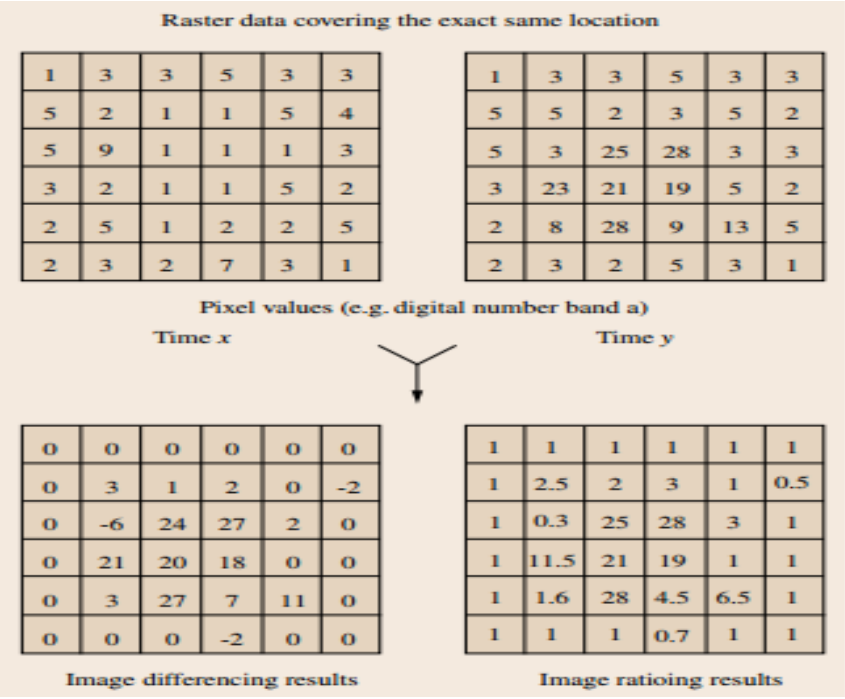


*Figure 6 – Simple Change Detection Calculations (Differencing vs Ratioing)*

Blundell (2006) used subsets of principal component analysis (PCA) images to perform object-based classification using the software Feature Analyst. The software considers both the spectral and spatial information of the pixel clusters through inductive learning algorithms (Blundell 2006). This improves the overall accuracy since the classifier uses the spectral information around the pixel to perform the classification as opposed to the pixel based approach that doesn't take any spatial context into consideration and analysis is done on a single pixel (YAO 2004). When comparing pixel-based classification vs object oriented classification, Weih (2010) produced 90.95% for pixel verses 94.47% obtained for object oriented classification when applying change detection in the Nothofagus forests (classifying between four classes). The authors were successful in isolating the two species of forests from water and non-forest features. For low to medium spatial resolution imagery, where objects and the pixel size are fairly similar in scale, the classification methods have shown to have similar accuracy. When high spatial resolution imagery is available, and objects consist of many pixels, that's where there's a dissimilarity in accuracy between the two methods. The aforementioned study is a good example of some of the limitations of pixel-based image classification techniques (Weih Jr 2010).

## 2.3 Multi-Criteria Decision Analysis (MCDA)

MCDA methods were found during the 1970s when critique arose of the traditional neoclassical environmental economics (Keeney 1976). The main weakness to the conventional neoclassical approach when regarding environmental and economic growths is that it can't cope effectively with external negative spillover effects (ex. Pollution) (Nijkamp 1980). Exploration of decision problems in a more multidimensional manner that included procedural elements followed the coming years. Multidimensional approaches such as MCE provides a more comprehensive comparison between alternative choices that take into consideration environmental and socio-economic factors (Carver 1991).

MCDA makes the use of decision rules defined either by mathematical means (choice function) or by a specific procedure function (choice heuristic) (Mabin 1999). MCDA offers a logical workflow for planning that evaluates alternatives in a systematic and transparent manner with the aim to find the most balanced and acceptable solution while clarifying concerns regarding disagreements/agreements of the criteria. The outcome of suitability maps is a GIS-based process that determines the significance of a specific use for the area of interest (Higgs 2006) . The sequence of steps involved with MCE is shown in Figure 7 which is the most commonly single objective assessment technique. The steps that make up the MCE is as follows:

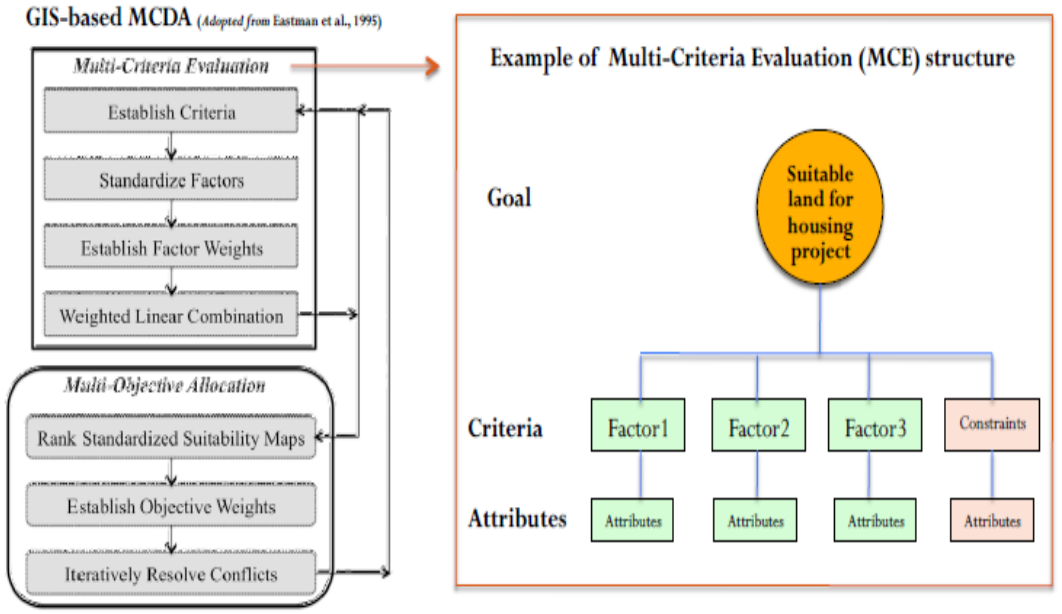


*Figure 7 – Example of Multi-Criteria Evaluation Structure (Eastman 1995)*

1) Set goal/ define problem

i. Has to be specific and measurable within a reasonable time-bound

2) Select the criteria (factors and constraints)

i. Should be measureable and the level of detail of the data should be decided (all roads vs only major roads)

3) Normalize criteria scores

i. Have a common scale for suitability values of factors for proper comparison (fuzzy membership functions)

4) Determine factor weights

i. Rate the factors using scale between 0 to 1 against each other, total summation equals 1 (lowest number = least important, highest number = most important, pairwise comparison)

5) Aggregate all criteria

i. Weighted linear combination is used to formulate the decision rule, as follows:

* All factors are combined into linear formula to produce a suitability map

Formula: $$S = \sum w_i x_i \times \prod c_j$$

Where:
S – is the composite suitability score
$x_i$ – factor scores (cells)
$w_i$ – weights assigned to each factor
$c_j$ – constraints (or Boolean factors)
$\sum$ -- sum of weighted factors
$\prod$ -- product of constraints (1-suitable, 0-unsuitable)

6) Validate

i. Compare with ground truth or reference data to test for reliability of the results

Multi-criteria evaluation (MCE) is a useful tool in choosing between alternative options regarding a specific objective. It can handle complex scenarios involving many criteria and factors. However, the downside to MCE is the subjectivity involved with choosing the criteria and choosing the factor weights, especially when applying a heuristic approach to ranking the factors. Openshaw (1989) used MCA to find suitable areas for radioactive waste disposal by the use of overlay routines within an area of interest via the implementation of weighted linear combination of the following four factors: geology, population distribution, conservation and accessibility (Carver 1991). Recently, a site selection for astronomical observation in Antalya province of Turkey was conducted by Koc-San (2013) using GIS data integrated with Multi-Criteria Decision Analysis. Eleven factors from three main categories were used: meteorological, geographic and anthropogenic. The weights of factors were decided through the analytical hierarchy process technique, to produce the most suitable locations.

# 3 STUDY AREA AND DATA

On December 26, 2004, an earthquake with a magnitude of 8.9 occured to the west of Sumatra Island of Indonesia. The earthquake in the middle of the ocean (tsunami) caused tidal waves up to 30m that struck twelve countries within the Indian Ocean. The 2004 tsunami was estimated to have released 1.1x1017 joules of energy which is equivalent to 26 megatons of TNT or 1,500 times the energy created by the Hiroshima atomic bomb (USGS 2010). Figure 8 shows the epicenter of the tsunami and the countries that suffered loss of lives and endured extreme damage, particularly settlements along the coast. The tsunami was one the most deadly disasters recorded in recent times with an estimated total damage of 15 billion dollars and over 300,000 people either missing or found dead (Matsumaru 2012).

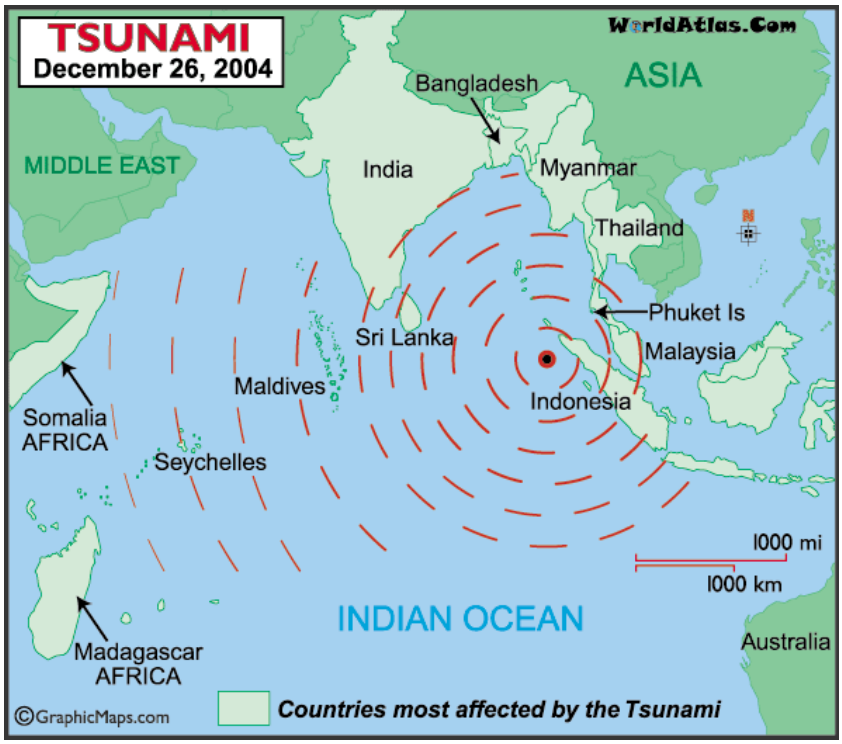


*Figure 8 – Epicentre of 2004 Indian Ocean Tsunami and Countries Affected (Worldatlas)*

The Study Area is Banda Aceh, Indonesia situated north-western tip of Sumatra Island at the mouth of the Aceh River (Figure 9). It is an important transportation and trading hub in the Eastern Indian Ocean with a population of 220,000. The city covers an area of 65km$^2$ and is home to many important landmarks for the Acehnese people of Indonesia. The 2004 tsunami

with tidal waves of up to 30m destroyed the whole city with total destruction of all infrastructure within 2 km of the coast.


*Figure 9 – Map of Banda Aceh, Indonesia*

## 3.1 Data

Two Landsat 5 satellite images around the disaster date of December 26, 2004 were downloaded from EarthExplorer (http://earthexplorer.usgs.gov). The images had some cloud cover to the northeast of Banda Aceh which was masked out and wasn't used for analysis. Table 1 below, provides further information on the images used.

| Acquisition Date | Sensor | Path/Row | Landsat | Number of bands | Radiometric Resolution |
|---|---|---|---|---|---|
| 21/12/2004 | TM | 131/56 | 5 | 7 | 8 bits |
| 22/01/2005 | TM | 131/56 | 5 | 7 | 8 bits |

*Table 1- Landsat 5 Satellite Imagery Properties*

Open Street Map (OSM) data was also downloaded from geofabrik (http://www.geofabrik.de/) for Indonesia.

### *3.1.1 Reference Disaster Map*

The International Charter's SERTIT agency produced damage assessment maps of Banda Aceh three days after the tsunami occurred (Figure 10). As part of the rapid mapping initiative, SERTIT failed to produce a damage map within the 12 hour set goal. SERTIT used Spot imagery with 2.5 meter spatial resolution and ground data to produce this damage map characterized into two groups, damage within urban areas and damage within rural/natural area. The damage is quantified into four groups from total devastation to no/slight damage. This map will be used as the reference map to compare with the maps produced. Although this map is meaningful and easy to understand for non-GIS users, the three days it took for processing is concerning given the context of the disaster event. Right after a disaster event hits, time is of essence in order for maximize the human recovery phase. The field, local authorities can greatly benefit from a rapid generalized analysis that will provide an overview of the affected area similar to SERTIT's map to efficiently and effectively allocate emergency efforts within a short time frame. Keeping this in mind, a semi-automated method is proposed to create damage maps within a shorter time frame.

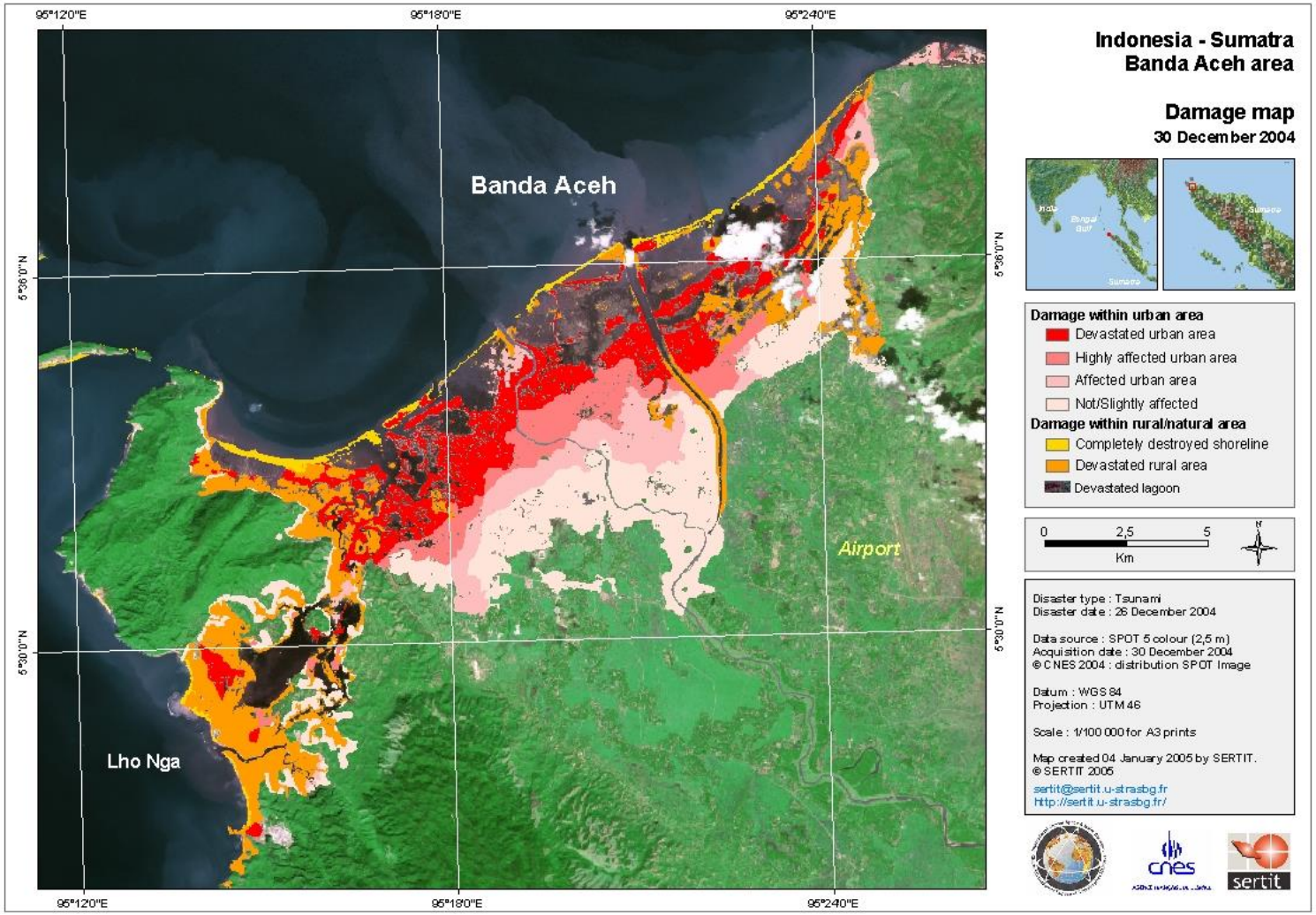


*Figure 10 – Banda Aceh Damage Map by SERTIT*

### *3.1.2 Reference Temporary Living Centres (TLC)*

There wasn't any reference data to evaluate the generated temporary housing center sites quantitatively. A UN map of temporary living sites after the 2004 tsunami in Banda Aceh can be seen in Figure 11. The map shows that most of the temporary living sites within Banda Aceh are located around the outskirts of the city with very high concentration on the south-eastern and north-western. Visual analysis will be conducted between the relative locations of the temporary living sites in the map and the ones obtained from MCDA to test if the factors chosen and the weights given were reasonable.

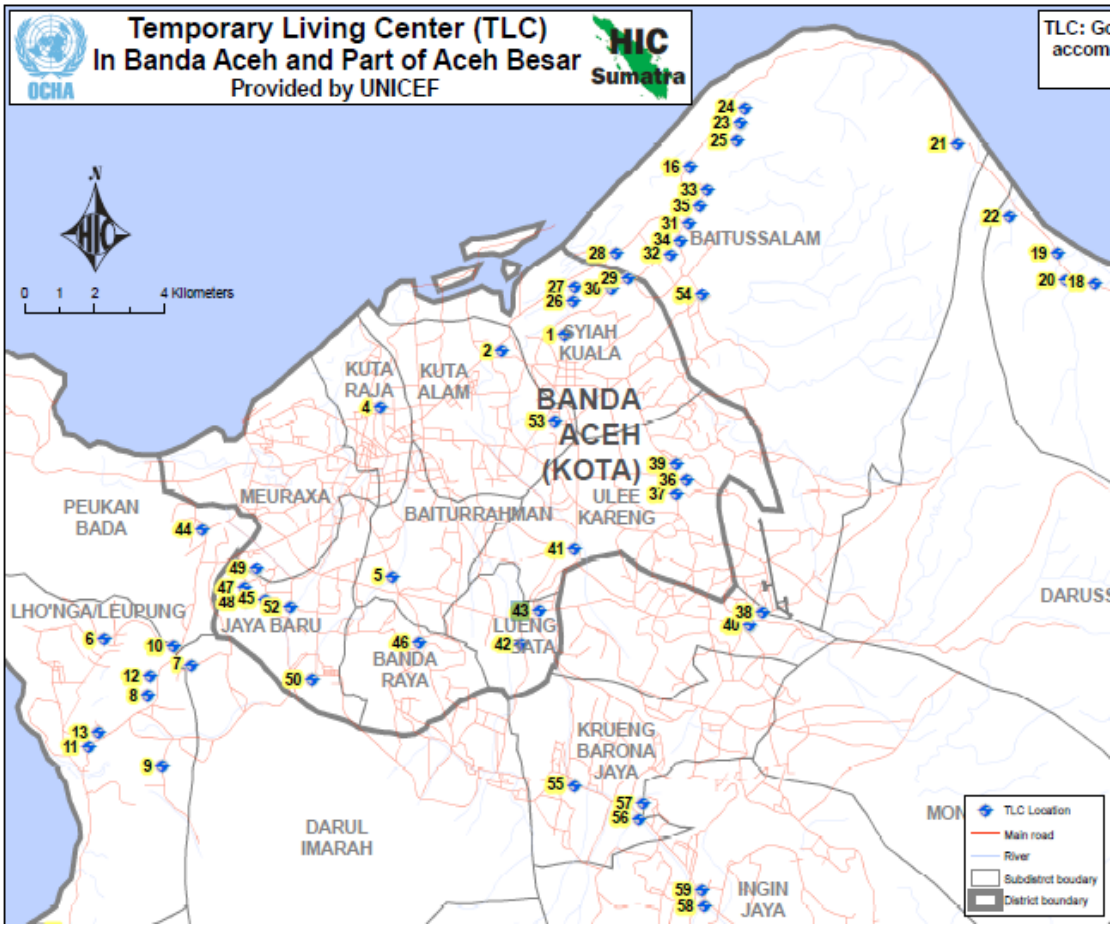


*Figure 11 - UN Temporary Living Centres (Reference Map)*

# 4 METHODOLOGY

The semi-automated workflow for creating disaster maps and temporary housing sites is illustrated in Figure 12. Image differencing and ratioing change detection is applied to pre and post disaster Landsat 5 TM satellite images based on city blocks created from the road network. Geometric classification is then applied to classify all the resulting change detection calculations into four classes and then compared against the SERTIT reference map. Error confusion matrix is then used to evaluate the overall and kappa accuracies. The most accurate map is then used with OSM data to compute Multi-Criteria Analysis in selecting the most suitable temporary housing sites for displaced individuals.

The semi-automated workflow consists of eight tools that follow a sequence with vital visual analysis steps in between some processes. Ideally, the whole workflow was planned to be implemented in Feature Manipulation Engine (FME), since the geoprocessing speed is faster than ArcMap, but due to the fact that ArcMap already has some predefined tools that perform some essential geoprocessing steps of the workflow as well as a better interface for visual analysis, it was decided to incorporate it into the workflow. The workflow requires the use of both ArcMap's Modelbuilder and Python capabilities as well as FME's visual scripting. This is due to the fact that both applications have their strengths and weakness, where ArcMap has specific tools for some processes as well as better visualization and FME is more efficient and powerful with regards to complex processes especially when dealing with big data. One of the goals of creating this workflow was to minimize the time required to create the damage assessment maps by means of incorporating the use of both the applications. Overall, ArcMap is used to create five tools and all visual analysis of results is done within ArcMap, and three tools are created in FME. The workflow is broken up into four main parts:

1. Creation of blocks
2. Zonal statistics and change detection procedures
3. Map creation and accuracy evaluation
4. Multi-criteria analysis

The workflow was designed to offer accurate damage results within a short time frame in order to maximize emergency response efforts. The workflow makes two assumptions for detecting change:

1. The extent of change in a pixel value from pre to post imagery is correlated with damage disregarding other factors that may have influence
2. Positive or negative change is considered the same (absolute value)

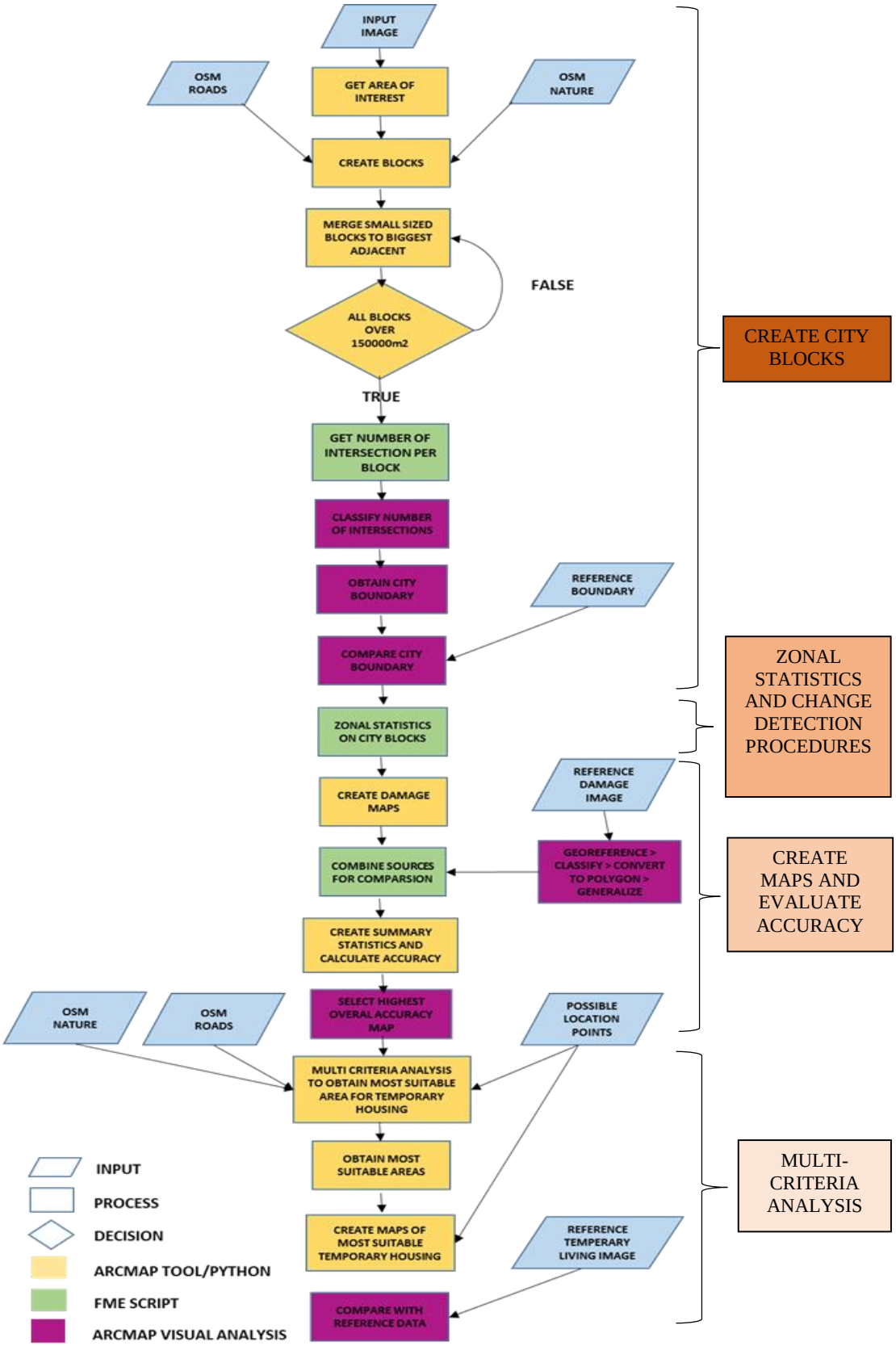


*Figure 12 – Overview of Semi-Automated Workflow for Damage Assessment*

## 4.1 Pre-Processing

### *4.1.1 Image*

Usually geometric, radiometric and atmospheric corrections are applied when performing change detection on multi-date imagery. Geometric and atmosphere corrections were ignored due to the fact that area of study was cloud free and the Landsat imagery was already geometrically corrected. Radiometric correction is crucial for change detection analysis as it adjusts for the difference in atmospheric and sun geometry conditions. When the time between the images is minimal and taken in the same season, sometimes radiometric corrections can be ignored because the change is minimal. Song (2001) argued that radiometric correction isn't needed when using maximum likelihood classifier or post classification on a single date or on classification of multi-date composite imagery that is placed into a single dataset. A quick test using linear normalization was applied and the difference between the normalization values and the true digital number was minimal, so it was decided to ignore applying the correction. Overlooking all the corrections and working with the raw image simplifies the workflow and quickens the process which can be indispensable for rapid mapping of an area affected by a disaster.

The Landsat image was clipped to Banda Aceh and the surrounding areas. Figure 13 shows an area of around 70km$^2$ being clipped from the original Landsat imagery. The goal was to assess the damage of Banda Aceh so all the other more natural surrounding areas were clipped out.

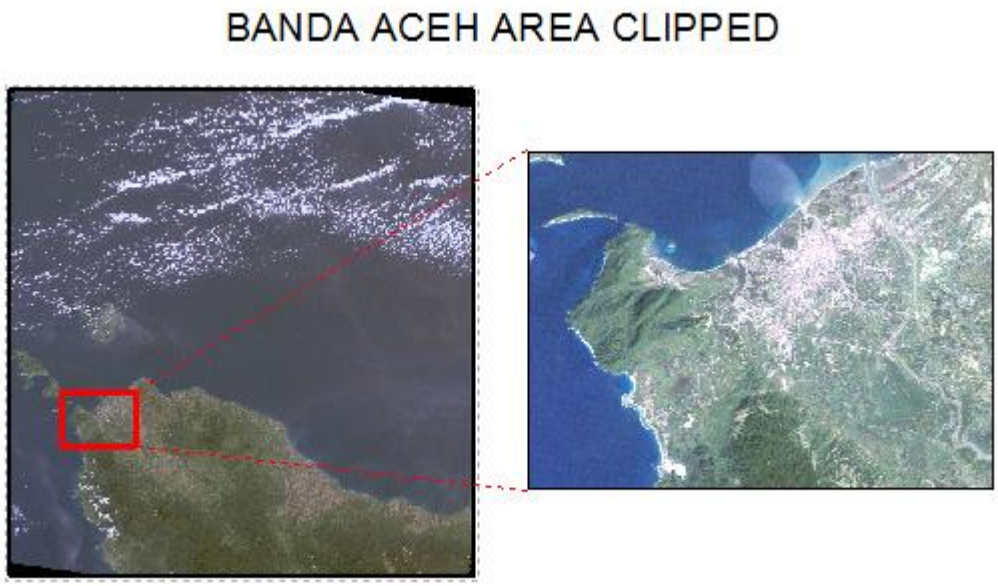


*Figure 13 – Clipped Landsat Imagery to Banda Aceh, Indonesia*

### *4.1.2 Open Street Map Data*

OSM data was downloaded for Indonesia and clipped to the same extent of the image. The features used from the OSM dataset are as follows: OSM roads (linear), OSM nature (polygons) and OSM buildings (polygons). The OSM nature was filtered to only keep: Forests, parks, and water bodies (Ocean and River). The OSM building file was also filtered to only keep buildings that were easily accessible/recognisable and large enough to accommodate a relatively large number of people: Hospitals, school, mosque, church, place of worship, police station. The area for the OSM buildings were then calculated and the polygons converted to points. The OSM data was also cleaned to account for inconsistent naming of some feature types and to diminish the effects of noise and redundant data.

## 4.2 City Block Creation from Roads

ArcMap is used for the first phase of the workflow which leads to the development of the city blocks. The artificial city blocks are created from the road network and the OSM nature file is firstly used to create the coastline and disregard everything inside water as well as delete from the resulting polygons areas that are occupied by forests and parks because the main goal of the study is to evaluate urban built-up damage.

The first step is to create a blank polygon that covers the raster image extent, which is executed by the raster to polygon tool. All the values are transformed to one unique value using the raster calculator with the intention of obtaining a constant uniform polygon. Once the plain polygon is created, the roads are inputted into the split polygons with lines tool in order to create the blocks. The polygon areas intersecting the nature file are erased to eliminate areas belonging to water and natural features from the study. The script sequence can be seen in Figure 14 as well as the tool prompt which requires the input raster image, the roads, the nature file and output file name.

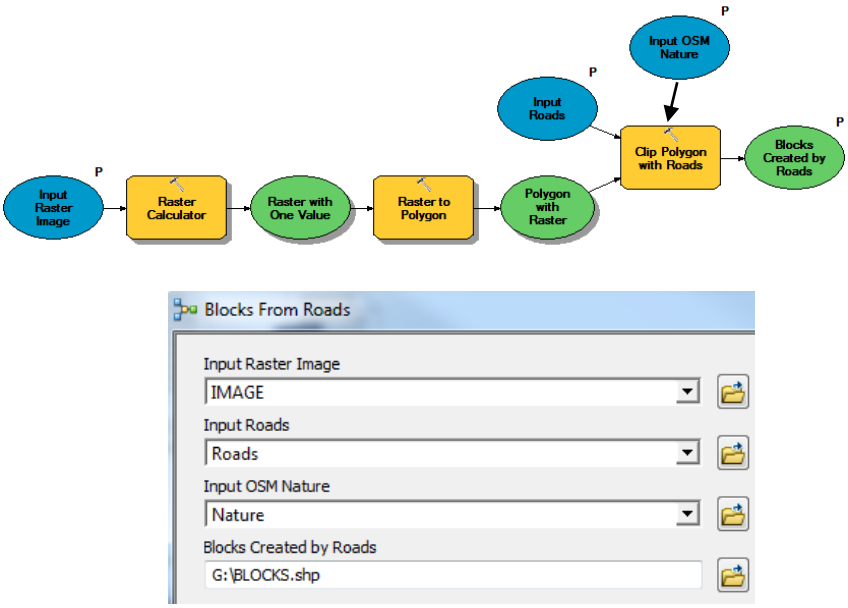


*Figure 14 – The Script Workflow of Creating City Blocks and Tool Interface*

In the area of study, the OSM roads were classified as mostly residential (approximately 90%), so the roads weren't filtered before the creation of the blocks since the blocks would have been too large due to the loss of the network if the residential roads were to be taken out. With the residential roads included, many small irrelevant blocks will be created that at a small scale map such as the one that will be produced by this research will only add the "salt and pepper" effect which will make it harder to visually analyse patterns and locations of damage.

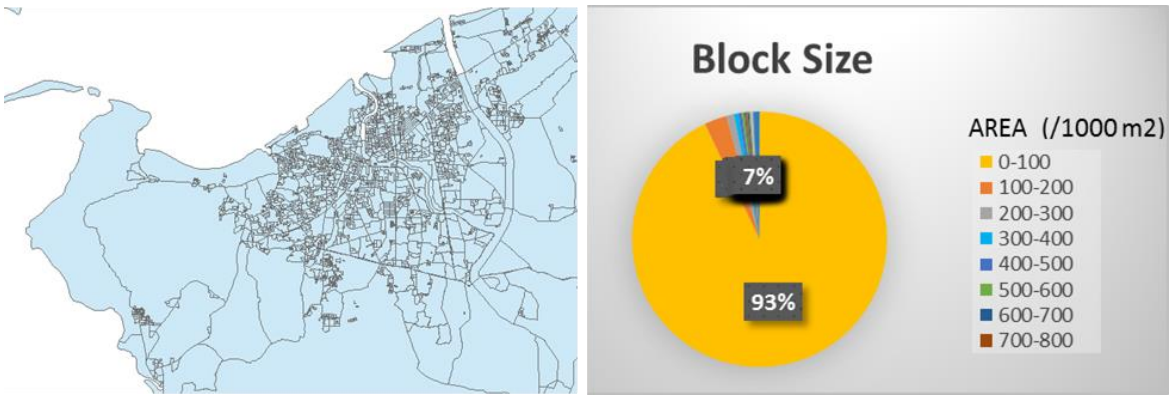


*Figure 15 – First Iteration of City Blocks and Block Areas*

Figure 15 shows the blocks created (left) and the size of each block. The majority of the blocks (about 93%) are under 100,000 $m^2$, indicating that most of the blocks are insignificant to the "big picture" or overall pattern and will only add uncertainly when visually inspecting the map. Through descriptive analysis coupled with visual analysis of the blocks, it was decided to merge all blocks under 150,000$m^2$ to the largest adjacent polygon. Since some of the small polygons

(under 150,000m$^2$) are surrounded by small blocks, the process had to iterate five times in order to ensure every block was over 150,000m$^2$.

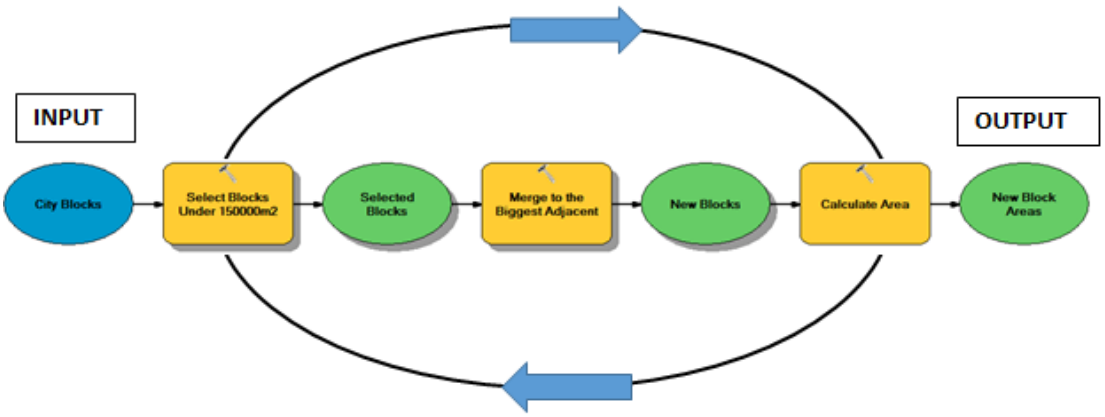


*Figure 16 – The Block Size Iteration Workflow*

The iteration is done in a python script within ArcMap, in which a while loop is used to run through the block size and execute the merge of blocks under 150,000m$^2$ to the largest adjacent until all blocks are over 150,000 m$^2$. The logic of the python script can be seen in Figure 16 in which three ArcMap tools are used to run the merging of blocks. The city blocks are introduced as the input, firstly each block with an area of under 150,000m$^2$ is selected using the select layer by attribute tool. Once the blocks under 150,000m$^2$ are selected, then the selected blocks are merged to the remaining blocks to form larger blocks. Then the block areas are calculated again, and the process is ran again until the count of the selection of blocks is 0. For this dataset, the script iterated five times in order to achieve polygons of over 150,000m$^2$.

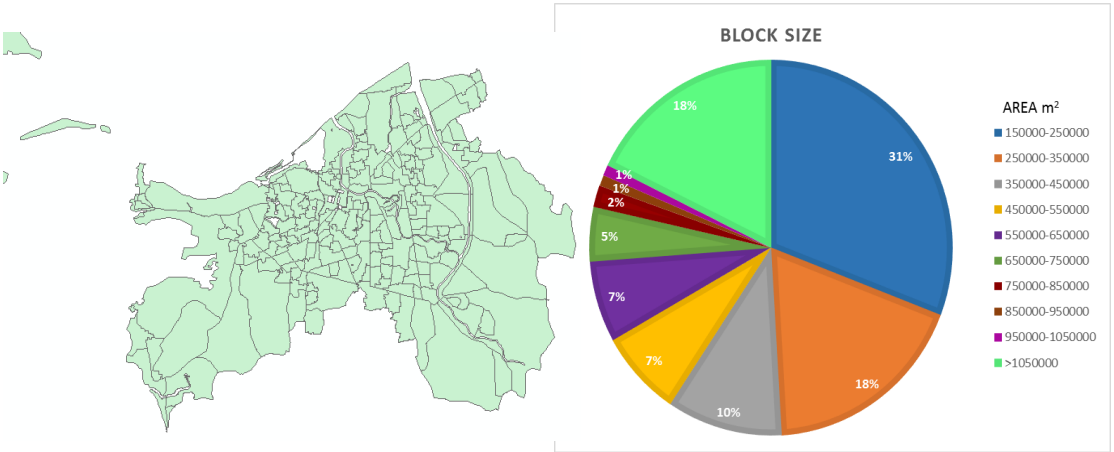


*Figure 17 – City Blocks and Block Size after Iteration Process*

The new city blocks created by the roads nature file can be seen in Figure 17. The size of the blocks are more uniform in around the city with larger blocks in the surroundings. The most prominent block size is between 150,000 to 250,000m$^2$. The city block area are also more even with over 75% of the blocks falling between 150,000 to 750,000m$^2$. The average size is just under 500,000m$^2$, with most of the blocks having areas around that mark. There are a few really exceptionally large polygons usually in the surrounding rural area, which will be eliminated from the study once only the polygons corresponding to the inner core (urban built-up) of Band Aceh are selected. The city block size are now ready for further analysis but first the city boundary of Banda Aceh needs to be obtained. One can assume that larger polygons are not part of the city limits due to the lack of roads infrastructure. To obtain the city limit and use only the blocks that fall within the city limit, the road network was used as a basis for delineation. The road network was clipped for each city block so that only the roads within each block was obtained. The number of intersections is then counted by creating a point at each intersection using the intersector transformer in FME. The point on area transformer is then used to group the points per block. Since some blocks are larger in size than others, using only the count of intersection won't be a reasonable indication for urban development. The number of intersection points is divided by the area to get a density value, which provides a better means of comparison. A new field is created with the density values for each block using the attribute creator transformer in FME. A new shapefile is created with the addition density field and the script workflow can be seen in Figure 18 as well as the tool interface.

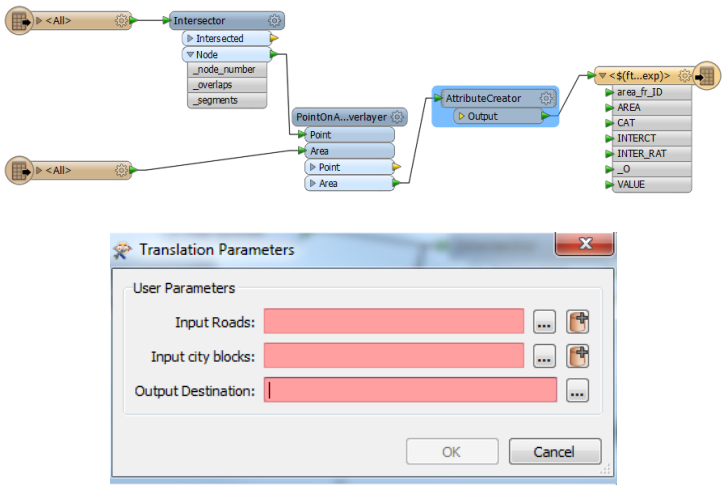


*Figure 18 – FME Script for Road Density and Tool Interface*

The shapefile is then added to ArcMap where it is classified automatically into three classes using geometric classification. The resulting classified map can be seen in Figure 19, where two classes seem to be closely related to road density and the third class just being the surroundings. Adding the road network on top of the classified map clearly shows the pattern

that seems to show the city boundary. The blocks within the two classes is then extracted and used as the city boundary. The city boundary is then tested against the satellite image of the pre event image and the outcome follows the boundary for the most part. This semi-automatic method for city boundary is used instead of post-classification because it requires less insight on the user part and it can be automated, whereas post-classification method of classifying urban areas from other classes will require training sites as well as post-classification analysis. Limiting the analysis to only the blocks within the city limits will reduce the influence of the other insignificant surrounding blocks into calculating the change statistics for disaster assessment.

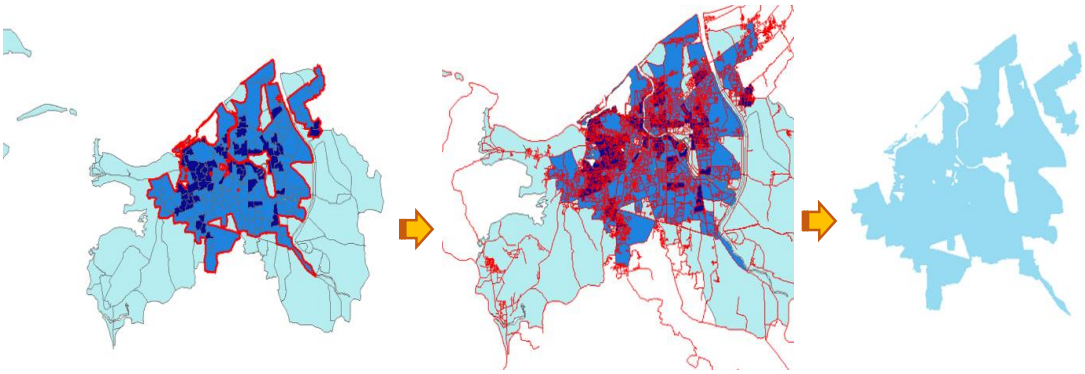

*Figure 19 – The Creation of the City Boundary*

## 4.3 Zonal Statistics and Change Detection

The city blocks are then used to run zonal statistics for the pre and post disaster images with change detection computed using two different approaches: image differencing and image ratioing. For change detection, image differencing and ratioing are the two most commonly used, simplest, efficient and most effective in terms of accuracy. Singh (1989) evaluated the most common change detection techniques in forest change. The simple techniques such as image differencing and ratioing out performed much more sophisticated methods such as principal components analysis (PCA).

A script in FME is implemented to calculate and organize all the zonal statistics for both images as well as calculating the differencing and ratio values between the images (Figure 20). FME

is a collection of integrated spatial ETL (extract, transform, and load) tools for data transformation/manipulation and data translation. FME geoprocessing works on feature by feature basis while ArcMap works on a feature-class by feature-class, which makes FME much more flexible and powerful when dealing with data. For example, in FME you can split the input features into different streams (serial or parallel) depending on defined conditions whereas in ArcMap, the whole feature class is treated at the same time or selected subset of the feature class. Instead of change statistics being done on pixel by pixel basis, it's done via a block by block basis. The script calculates the differences and ratios between the pre and post event imagery for all six bands of the Landsat 5 imagery as well the NDVI, NDBI and NDWI indices. The script calculates the max, min, standard deviation, range and mean for all blocks for each of the two images, taking the all the pixel values within the blocks rather than taking each pixel individually. Once the statistics have been calculated, then the differences and ratios are deduced on the same block from the pre and post disaster data. Due to the bulk of the data and some descriptive analysis, only the changes for the mean and standard deviation for each band and indexes are kept for further analysis.

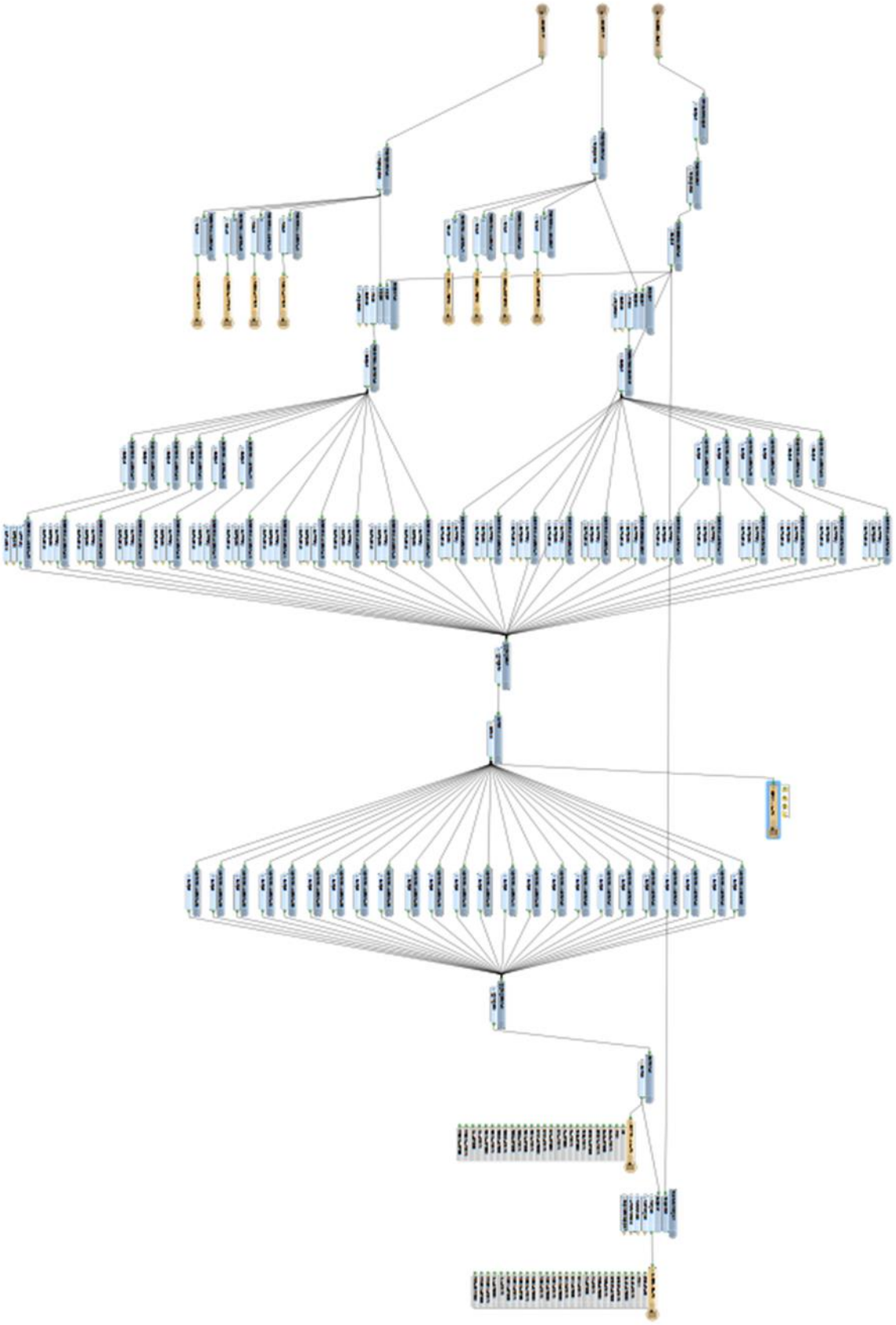

*Figure 20 – FME Script to Compute Change Detection*

The script can be broken down into three parts, with the first part seen in Figure 21, deals with the creation of the indexes, clipping the image to the boundary of the city limits and finally converting the information of each pixel into a point feature. Data is dealt with more efficiently and easier in FME using point features rather than raster data especially when doing zonal statistics manipulations. Every process is run twice, once for the pre-event image and the other for the post-event image in order to do the comparison and analysis at a later stage. The only requirements for this script are the pre and post image of the area and the city blocks. In this part of the script, eight raster files are created which comprises the four indices for each image. The information of the raster is also clipped to the area of interest and converted to points for further manipulations.

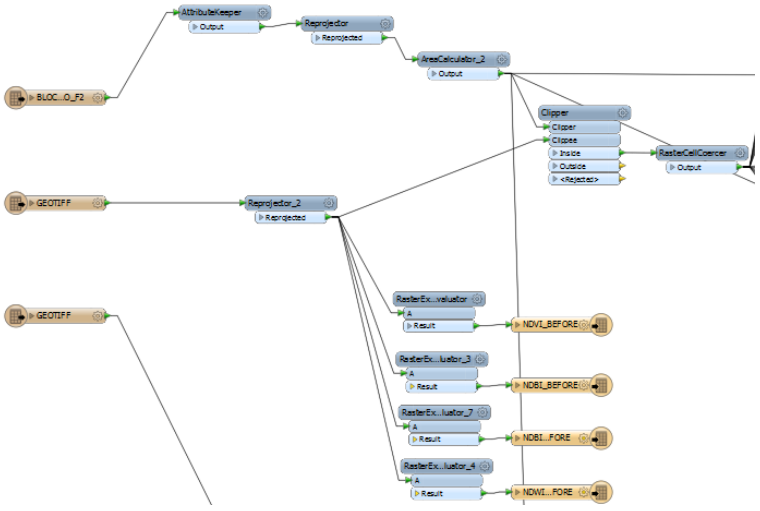


*Figure 21 – FME Script for Change Detection Calculation – Part 1*

The points now contain the values for each band, and using the statistics calculator, the corresponding bands are subtracted and divided for each point and then sorted by block (Figure 22). A DBF file is created, that includes all the raw data regarding the differencing and ratioing values of all the bands and indices for the following statistics: max, min, range, mean and standard deviation. The by-product DBF file contains all the raw data for validation purposes. All the final values can be traced back to the DBF to check for consistency. Two DBF files are created, one for differencing and other for ratio results containing 110 columns: 10 for each band/index and 5 columns for each corresponding before and after disaster image of which 5 columns relates to the maximum value, minimum value, range, mean and standard deviation for each block. Each block contains zonal statistics that will be used to compute change detection.

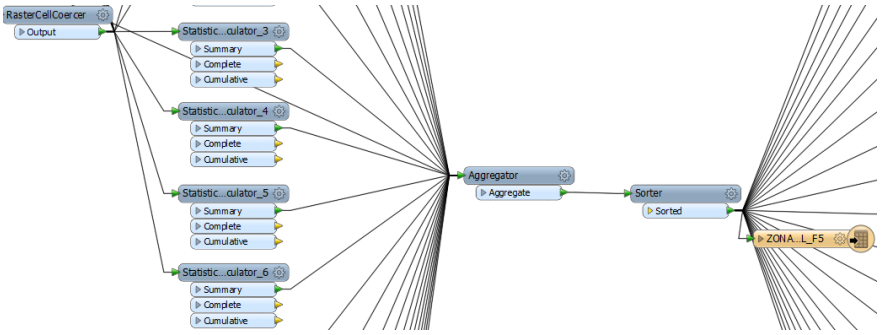


*Figure 22 - FME Script for Change Detection Calculation – Part 2*

In this part of the script, the statistics for before and after images are subtracted or divided to calculate the change variable for each block using the expression evaluator in FME. It was decided to apply the change detection methods on only the mean and standard deviation because it provided the most meaningful information about the blocks. Again another DBF file is created to verify all the fields were computed correctly and for consistency. The calculations are sorted by the block ID using the sorter tool in FME. The final product of the FME tool is a shapefile of the city blocks with added information on mean and standard deviation for each band/index. The different fields of the new shapefile can be seen in Figure 23, indicated by the green arrows. The values of the reference damage map by block that will be used to evaluate the accuracy is also added to the file using the feature merger. The shapefile is now ready to be classified for damage.

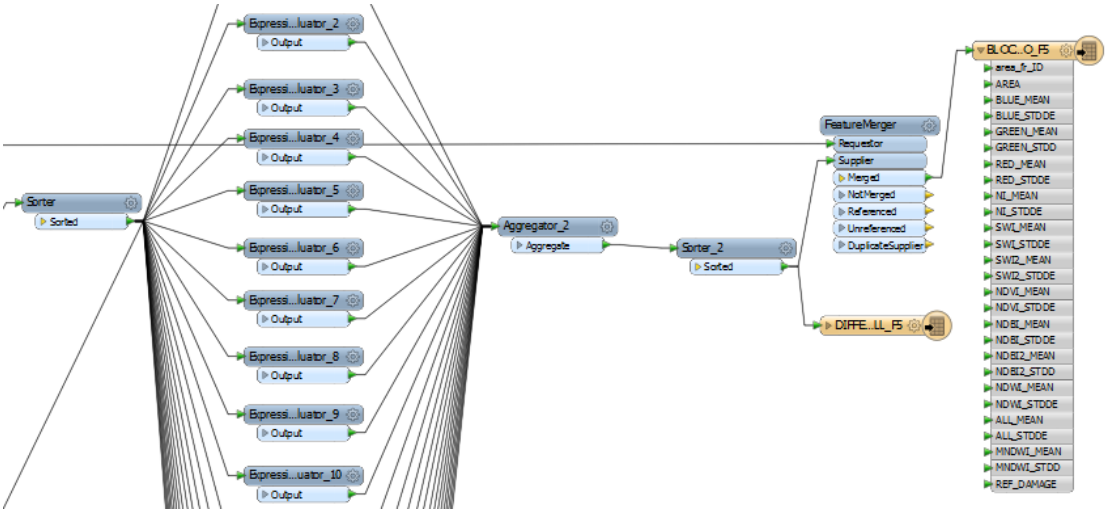


*Figure 23 - FME Script for Change Detection Calculation – Part 3*

## 4.4 Map Creation

The map creation was done in ArcMap using the reclassify tool in which geometric interval classification was applied independently on all band/indices change values with the purpose of obtaining four classes. The reason it's decided to have four classes of damage is to have direct comparison of results against the reference map which also had four levels of damage (Figure 10). Geometric classification was introduced by ESRI Geostatistical Analyst extension and is useful for visualizing not normally distributed continuous data. This method is designed for data that contains many duplicate values. Since the descriptive analysis showed the data not being normally distributed and having many identical values, it was decided to use this method for automatic classification. A vital step is setting the threshold boundaries for change vs no change which can alter the results considerably. It requires understanding the data and manual intervention and due to this being a semi-automated workflow, the threshold was automatically selected by the geometric classifier which may not guarantee the optimal result. Each of the blocks will be allocated into one of the automatically generated class based of the change values calculated in the previous step. The class with the highest change will correspond to the extreme damage and the lowest to no change will be assumed to be low damage. With eleven fields to map for each method (differencing and ratioing) plus the two statistics measures (mean and standard deviation), overall 44 maps were created to be evaluated with the reference map for accuracy. Figure 24 shows maps created from differencing of the six Landsat bands. The darker blue indicates more damaged blocks than lighter shades and the general trend makes sense indicating that the more damaged blocks are closer to the ocean except for the shortwave infrared maps which show random patterns.

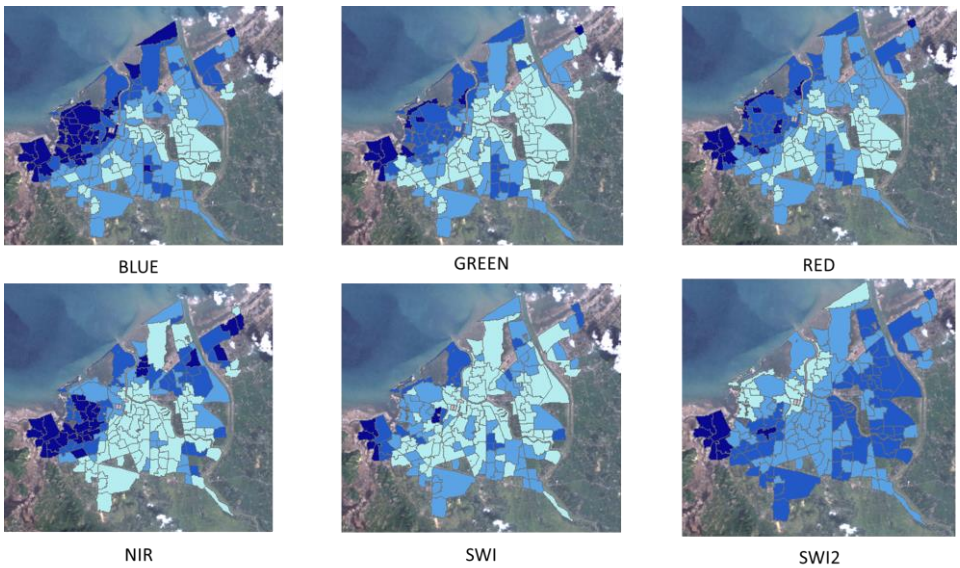


*Figure 24 – Varying Damage Patterns from Six Bands of Landsat (Image Differencing)*

## 4.5 Multi-Criteria Decision Analysis

Safe land is a scarce resource during a disaster, so the selection for the best temporary housing site has to take many things into consideration. Decision making of how the land should be used is not an easy task as a result of people's different priorities, goals, interests and concerns. Spatial decision problems usually have many alternative solutions which at times are in conflict with each other. Since many possible options and criteria are evaluated by many individuals, it's only expected that the preferences and objective ranking of many are inconsistent. GIS-based Multi-Criteria Decision Analysis (MCDA) is an effective tool in aiding the decision making process between alternatives. MCDA provides the mechanism for configuring decision problems by evaluating alternatives to essentially rank and prioritise them. Combined with GIS data this adds a spatial component that can principally help decision makers make better and more informed decisions.

MCDA is used to find the most ideal temporary housing sites in Banda Aceh. The following factors were used: proximity to water, proximity to roads, building size and the created damage map. Only the water features (river and ocean) from the OSM nature file were selected and main roads (primary and highways) selected from OSM roads for analysis. Once the factors were decided, the criteria scores had to be normalized to have a common scale of suitability in order to compute suitable comparisons. Figure 25 shows how the factors were normalized from a scale of 0 (least suitable) to 10 (most suitable). As building size increases, the suitability also increases because bigger space can house more displaced individuals. For continuous data, the data was reclassified into 10 classes and each class assigned a suitability value. The distance from water bodies also follows the same trend of suitability due to the fact that with a tsunami, flooding occurs throughout and it's more likely around water bodies therefore it's more suitable away from water. The suitability decreases with distance from main roads because main roads are vital for the transportation of emergency supplies such as medical equipment, food and other basic needs so for accessibility purposes it's more suitable to be closer to these roads. For categorical data such as the damage map, the suitability value is assigned using the same scale. The areas that are totally destroyed are clearly least suitable and areas with lower damage more suitable.

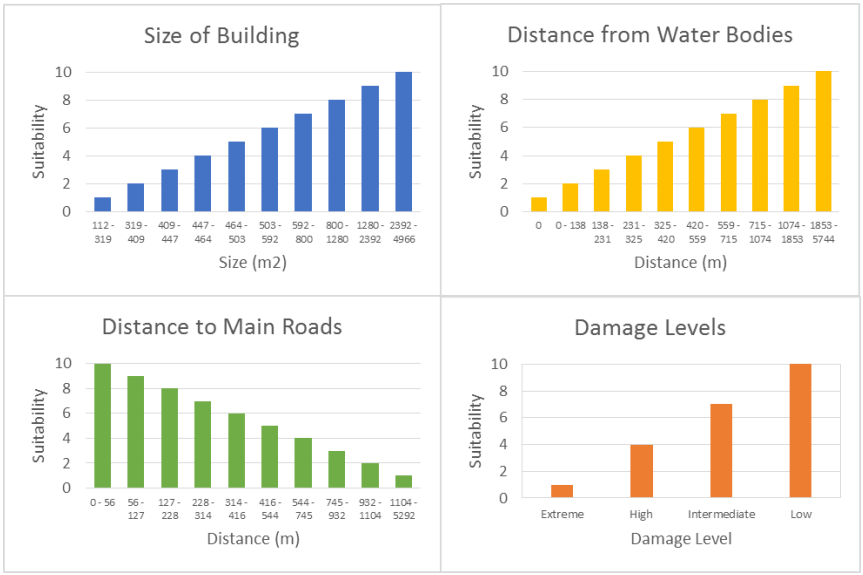


*Figure 25 – Normalized Suitability Scores for Each Factor*

The pair-wise comparison method was implemented with the aim of obtaining the weights of importance for each factor. To diminish the effects of biases, the importance of each factor against another factor was evaluated by three experts and normalized to 1 (100%). The normalized percentage of importance for each factor by the three experts can be seen in Table 2. All three experts had the same census with different variations, with the damage map being the most important and building size being the least important among the factors. Then the average of all three experts were calculated and the final weights were obtained for the linear combination formula to aggregate all the criterias. The damage map will have the most importance with 50% followed by the proximity to roads and water (20%) with building size being the least important (10%)  Experts are defined as individuals with over five years of experience in the domain of GIS.

| | Damage Map | Proximity to Water | Proximity to Roads | Building Type & Size |
|---|---|---|---|---|
| Expert 1 | 40 | 25 | 25 | 10 |
| Expert 2 | 45 | 25 | 15 | 15 |
| Expert 3 | 65 | 10 | 20 | 5 |

| FEATURE | WEIGHT (%) |
|---|---|
| Damage Map | 50 |
| Proximity to Water | 20 |
| Proximity to Roads | 20 |
| Building Type & Size | 10 |

*Table 2 - Expert Weights Given and Final Average Factor Weights*

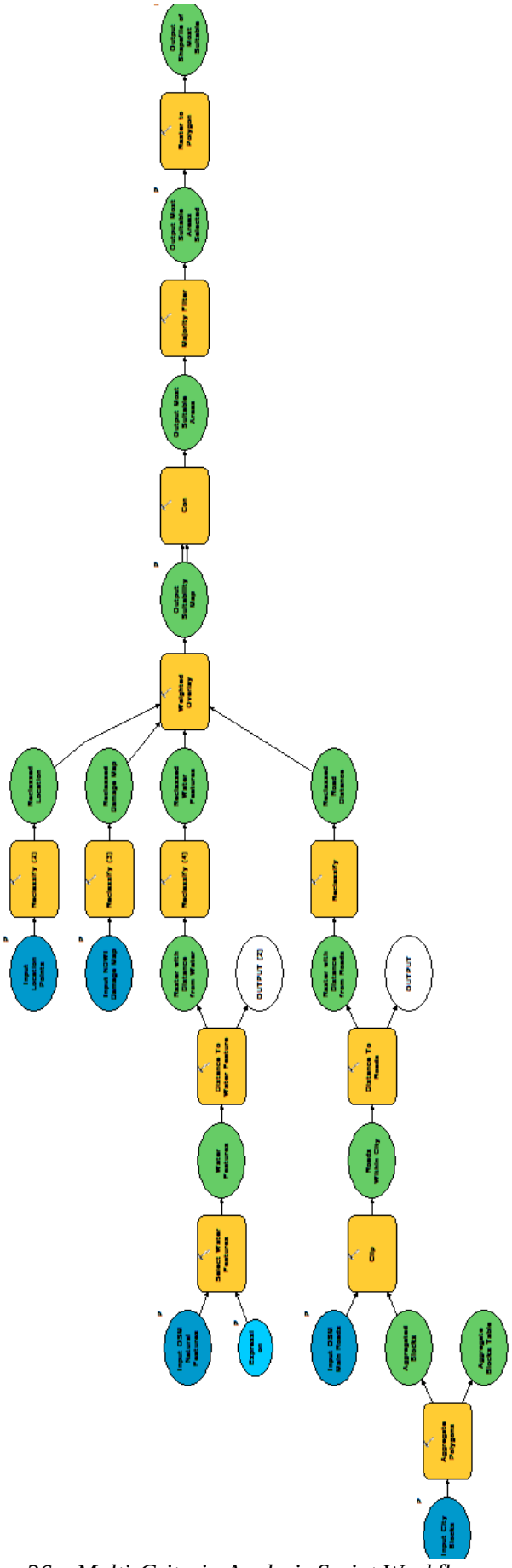

*Figure 26 – Multi-Criteria Analysis Script Workflow*

The MCDA tool was created in ArcMap and the workflow is shown in Figure 26. For the roads and water the distance is calculated first then reclassified into ten classes. After all the factors are reclassified the weighted overlay is used to signify the importance of each factor and by weighted linear combination, a suitability map is created (Figure 27). Then the highest suitable areas (suitability of 9 and 10) are towards the south of Banda Aceh away from the ocean and extreme damage areas. The highest suitable areas are selected and the building points within the suitable areas are chosen as the most suitable for temporary living sites for displaced individuals.

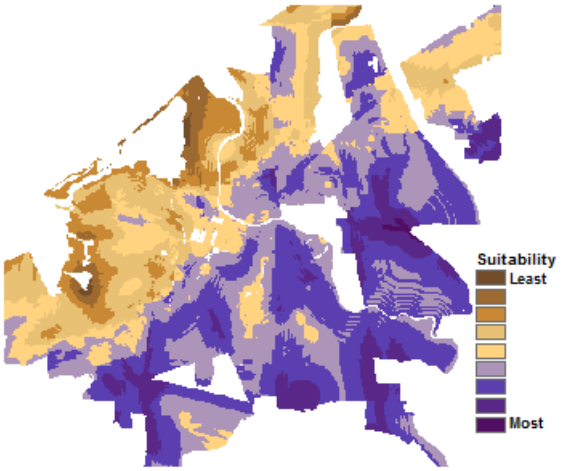


*Figure 27 – Suitability Map for Temporary Living Centre created by MCA*

The tool interface is shown in Figure 28 below.

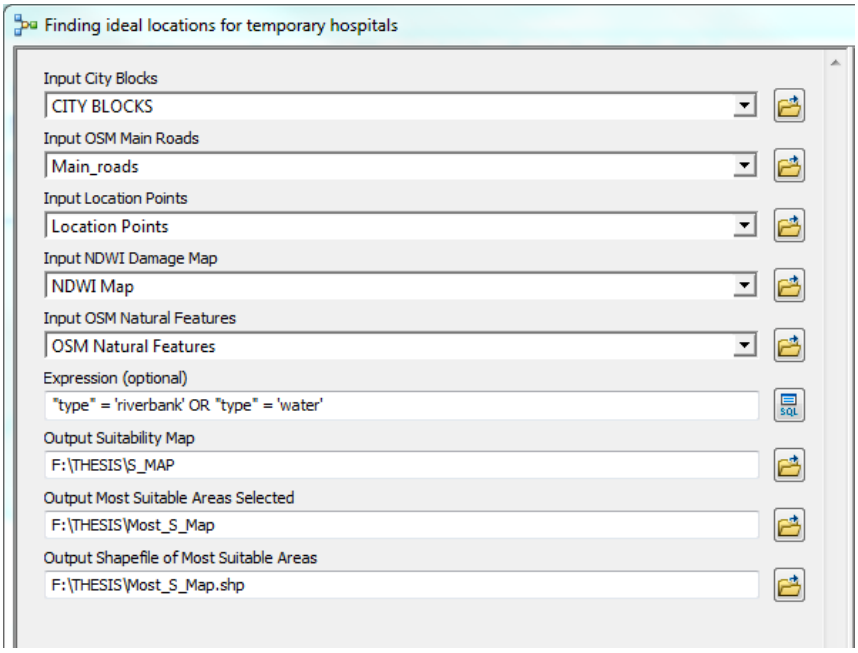


*Figure 28- Finding Ideal Locations for Temporary Living Centres Tool Interface*

## 4.6 Accuracy Assessment

### *4.6.1 City Boundary*

The city boundary created from road intersection density is assessed using two methods. The city boundary is a critical step because it selects the blocks within to apply change detection, therefore ensuring its acceptable is vital. Firstly, visual analysis on the city boundary overlaying the pre-event image is undertaken to assess if the city follows the urban outline of Banda Aceh. Figure 29(a) shows the city boundary on the pre disaster image, the outline appears to follow the urban areas of Banda Aceh generally well with some natural areas surrounding the south and northern side. This can be attributed to the fact that the blocks are artificially derived from the roads: where there are fewer roads (outskirts of the city), the blocks tend to be larger and less accurate.

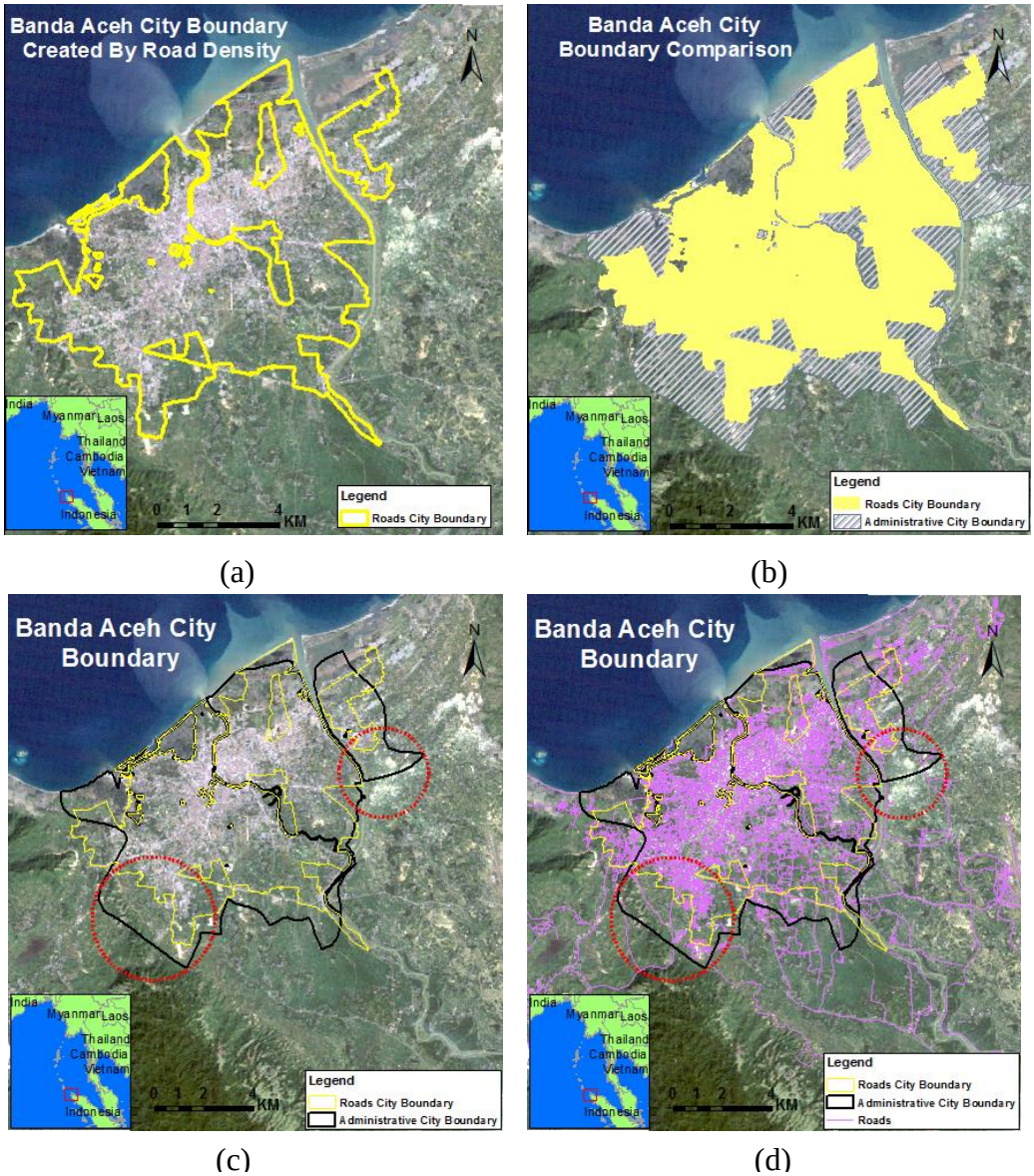


*Figure 29 – City Boundary Obtained from Roads Compared with Administrative Boundary*

The acquired city boundary is compared against the administrative boundary of Banda Aceh from 2014. Figure 29(b) shows that the administrative boundary covers about 26% more area than the acquired boundary from road density. Figure 29(c) shows the two boundaries against 2004 imagery which shows that the road city boundary follows the urban areas (indicated by colours other than shades of green) more closely. The areas highlighted by red circles are areas of most variation between the two boundaries, but one can visually observe that urban development is minimal in those areas. Figure 29(d) shows the boundaries with the roads also overlaid, which again shows that there's no indication of urban development in the extra areas included in the administrative boundary demonstrated by the low density of roads in the highlighted areas. The disparity between the two boundaries can be attributed to two key factors. Firstly the administrative boundaries include surrounding green areas and not only the densely populated areas. Secondly Banda Aceh had a population of 219,070 people in 2000 compared to 235,245 people in 2014 which is almost a 10% increase. The possibility of the city expanding in the surrounding areas of Banda Aceh is high. The city also received 7 billion dollars of aid from over 700 domestic and international organizations which could have also led to many urban development projects around the inner core of Banda Aceh to accommodate the increasing population. Due to the factors discussed above, the city boundary derived from road density was used as it provided a better outline of the urban areas of Banda Aceh.

### *4.6.2 Disaster Maps*

Overall, 44 disaster maps are produced using six Landsat 5 TM bands and specific indices that highlight vegetation, water and built-up areas. The maps produced show different patterns depending on the band/index used and the method of change detection applied so it is essential to evaluate the results with the aim to observe the best band/index for mapping urban damage from the 2004 tsunami occurring in Banda Aceh and to conclude which method is better for change detection. SERTIT, a rapid mapping agency operating under the International Charter initiative produced a damage assessment map using SPOT imagery three days after the disaster occurred. The product is a map in JPEG format so for it to be used as a reference map for direct comparison, it had to be georeferenced and rectified to the imagery. The reference image is clipped to the area of interest and six control points are used to georeference the reference image to the satellite imagery using ArcMap's georeferencing tool. Once the images are aligned, the data of the reference image has to be vectorised. Since the reference image is classified into four levels of damage using distinct colours, supervised classification is applied and the

resulting raster image is vectorised and generalised to only keep the four damage levels. Figure 30 shows the reference image and the resulting generalized vectorised damage.

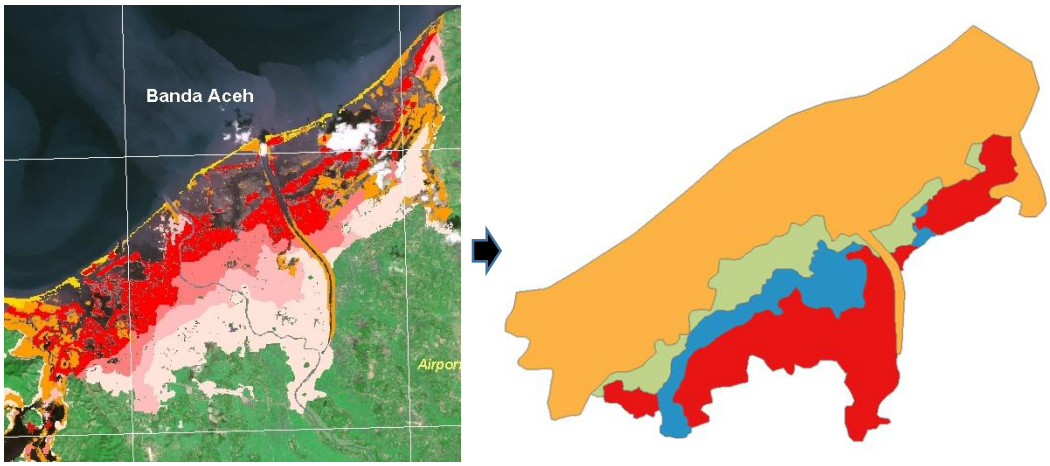


*Figure 30 – Vectorization of the Reference Damage Map*

The new shapefile with damage levels has to be divided into the same city blocks as the ones created from roads in order to perform direct comparisons and then compute accuracies. A FME tool is created to pass the reference damage level as a new field in the city blocks file with all calculated damage results. The reference data has to be organized to have a damage value for each block. The reference data is clipped by the city blocks and the corresponding damage value was passed on. Around 70% of the blocks are within one damage level so it was a direct transfer of value and for the other 30%, a majority filter is applied to count which level occupied more and that value was transfer to the block. Figure 31 shows the FME workflow and the user interface which requires two inputs (reference map and city blocks) and destination of the new file.

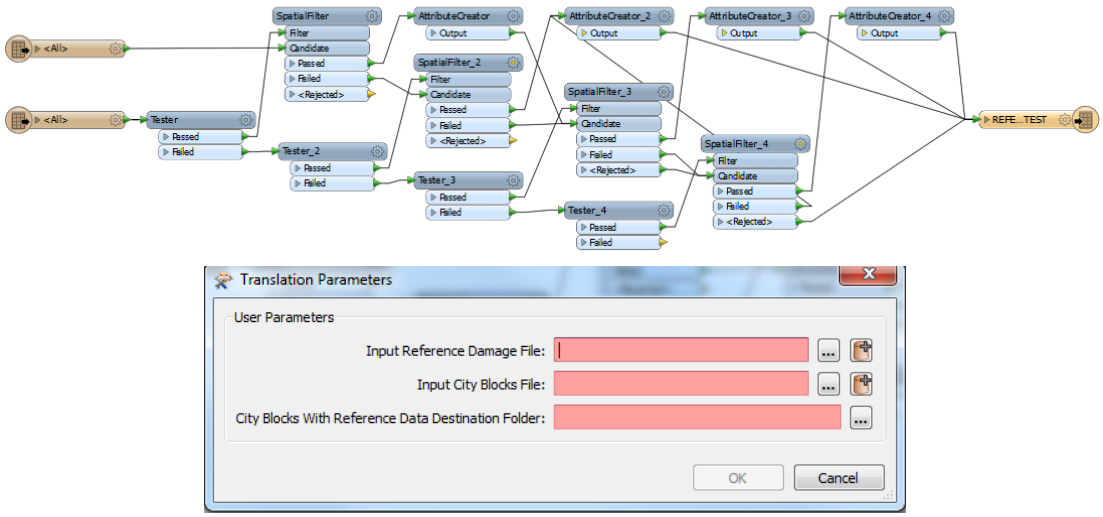


*Figure 31 – FME Script to Transfer Reference Damage Data to Blocks and Tool Interface*

The result of the tool is seen in Figure 32, where the values of the reference data are now transferred to blocks. The new file now has the four damage levels from the reference data plus 44 classified damage levels. The damage is classified into the following levels: Extreme, High, Intermediate and Low. Accuracy assessment can now be evaluated on the blocks.

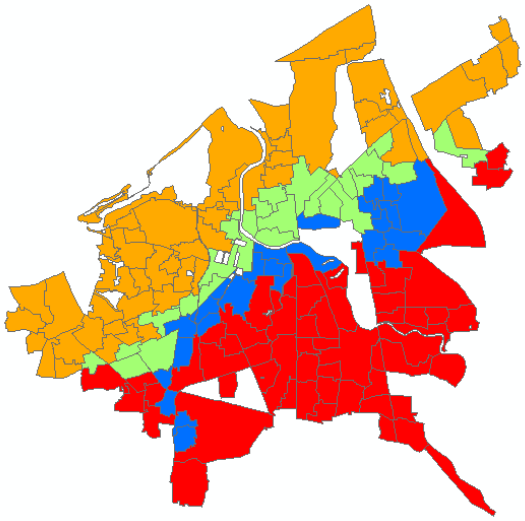

*Figure 32- City Blocks with Reference Damage Data*

### 4.6.2.1 Accuracy Measures

Confusion error matrix is a way of evaluating the reference truth data against the classified values in order to the see how well the classification symbolizes the real world. The confusion matrix is obtained by comparing each of the class and location of a block in the classification image with that of the corresponding one in the reference image. Each row of the confusion matrix represents the categorized map classes and the columns represent the reference truth class. The values in each columns indicate how the classified image labeled against the reference truth blocks (Macleod 1998). The confusion matrix provides some valuable error statistics which is evaluated by comparing the produced maps against a reference truth map. Some of the error values calculated using the confusion matrix are the overall accuracy, kappa coefficient, producer accuracy and the user accuracy.

The overall accuracy is obtained by dividing the total number blocks from the total number of blocks correctly classified (diagonal) in the error confusion matrix. The reference image outlines the true or right class of the blocks. In a confusion matrix, the correctly classified blocks run diagonally, and the number indicates the blocks of the classified class that matches with the reference truth class. The total number of class is acquired from the sum of all the reference truth classes. Producer's accuracy is an indicator of how well a certain block can be

classified. Producer's Accuracy is a measure of omission error which demonstrates a certain feature in the reference truth image is not classified the same feature in the classification. User's accuracy is the likelihood of a block class on the map representing the same class on the ground. User's Accuracy is a measure of the commission error which signifies when a block states the occurrence of a feature which in truth is absent (Morisette 2000).

Another indicator of accuracy assessment is the kappa ($\kappa$) coefficient which is a discrete multivariate measures the agreement between the reference truth values against the classification map. The kappa coefficient is said to be more robust than a simple agreement calculation since it takes into reason the agreement arising due to chance. The kappa coefficient takes the observed agreement (overall accuracy) and subtracts by the agreement due to chance and divided by one minus the agreement due to chance in order to standardize the results. The Kappa coefficient ranges from 0-1, with one representing perfect agreement and zero expressing zero agreement. Kappa coefficient values of greater than 0.80 represents strong agreement, 0.4 to 0.8 is mediocre agreement and under 0.4 is poor agreement (Kraemer 1982). The formula is expressed as follows:

$$\kappa = \frac{N \sum_{i=1}^{n} m_{i,i} - \sum_{i=1}^{n} (G_i \, C_i)}{N^2 - \sum_{i=1}^{n} (G_i \, C_i)}$$

Where :

- i is the class number
- N is the total number of classified pixels that are being compared to ground truth
- $m_{i,i}$ is the number of pixels belonging to the ground truth class i, that have also been classified with a class i (i.e., values found along the diagonal of the confusion matrix)
- $C_i$ is the total number of classified pixels belonging to class i
- $G_i$ is the total number of ground truth pixels belonging to class i

# 5 RESULTS AND DISCUSSION

## 5.1 City Blocks

Figure 33 shows the final city blocks within the metropolitan boundary and block size compared to the average. Overall, there are 159 blocks varying in size from 153,000m$^2$ to 2,840,000m$^2$ derived from the original 2,915 blocks varying in size from 1m$^2$ to 215,000,000m$^2$. The aim is to have block sizes big enough to have meaningful influence in the small scale map pattern, at the same time not adding noise that might be visually displeasing and not too large to take into account the heterogeneity of the landscape. The total study area also decreased significantly from originally being around 612km$^2$ to around 70km$^2$ when only the blocks within the city boundary are selected. This helped limit the calculated change to only urban areas. Setting of a minimal block size which led to the aggregation of small blocks and limiting blocks only within the city boundary helped define the blocks to measureable comparable units at this scale. Figure 34 shows that the majority of the blocks are have an area close to the average. The gap within the blocks are created from erasing overlapping features from the OSM nature file. The selected features are rivers, parks, forests and ocean. The aim is to measure change resulting from urban and eliminating these features provides better approximation of urban change rather than other factors. There is also a gap of missing blocks in the northeastern part of the map, those blocks were eliminated due to close proximity to clouds. With the purpose of minimizing the effects of cloud cover and cloud shadows, the blocks were eliminated.

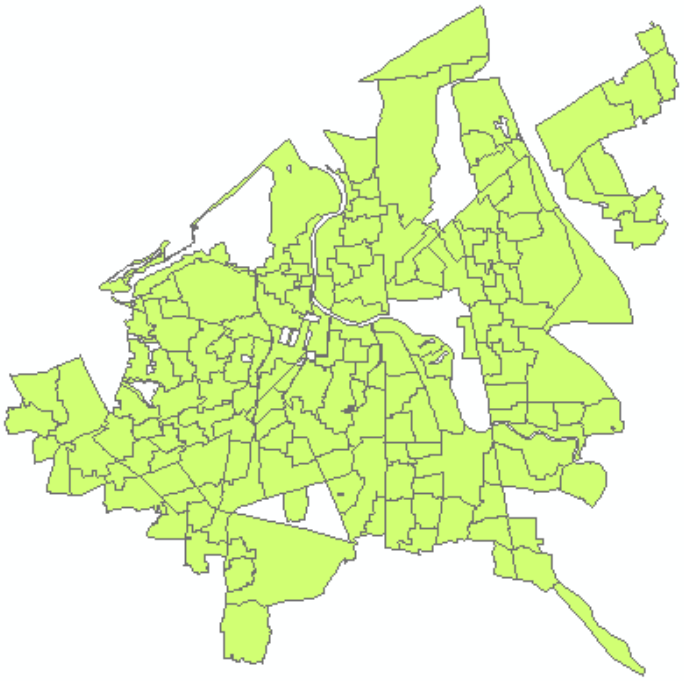

*Figure 33- Final City Blocks*

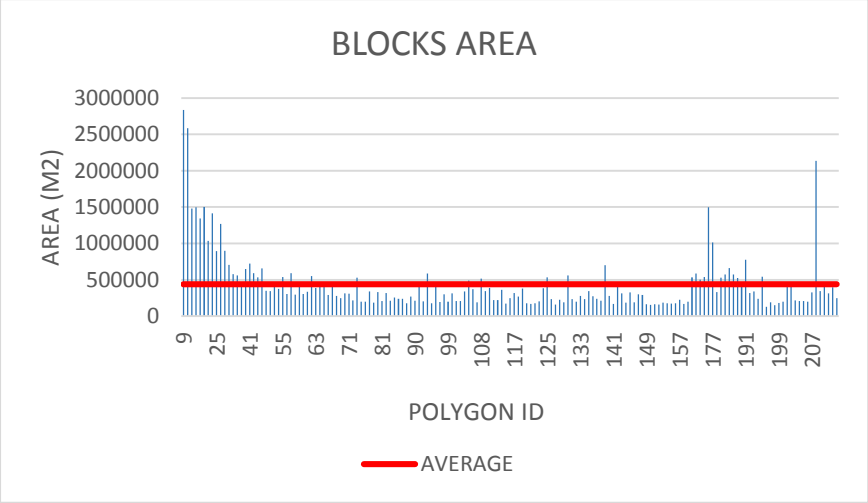


*Figure 34 – Final Block Size Compared Against Average*

## 5.2 Accuracy Assessment

### *5.2.1 City Boundary*

Figure 35 shows the outline of the final city boundary used for Banda Aceh shown in red. The boundary captures most of Banda Aceh urban built-up area and was used to extract the blocks only within this boundary so the change detection differences or ratios in which the disaster maps are created from are only from urban change and not affected from other LULC features.

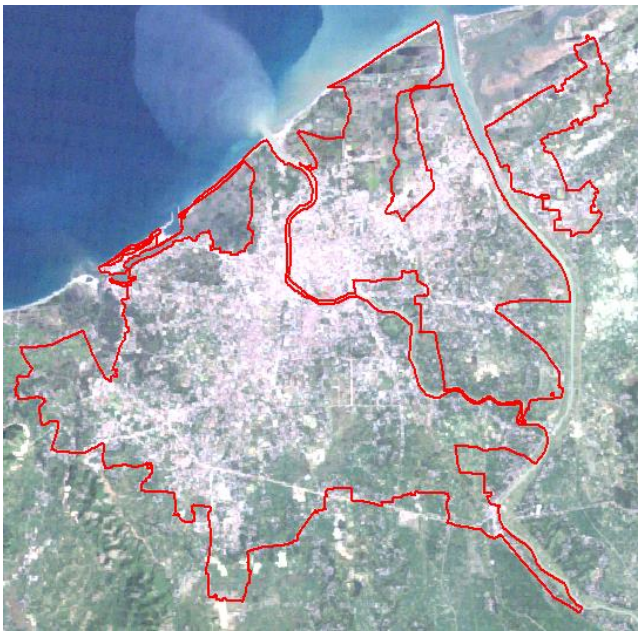

*Figure 35- Final City Boundary Derived from Roads*

### *5.2.2 Disaster Maps*

The disaster maps were evaluated for accuracy using error confusion matrices. All 44 classified maps are compared against the reference map using frequency statistics that matches unique field values with the number of occurrences between the two unique fields. Once the frequencies are calculated then the formation of error confusion matrices are produced for all 44 classified maps. The confusion matrix of the NDWI differencing map can be observed in Table 3. The overall accuracy (in yellow) is calculated by summing the numbers associated with matching level of damage between reference map and classified map which ran diagonal (in green) and dividing by the total number of blocks (in blue). The user's and producer's error is also calculated for each damage level as well as the 95% confidence interval.

| | | CLASSIFIED MAP | | | | | | |
|---|---|---|---|---|---|---|---|---|
| | | EXTREME | HIGH | INTERMEDIATE | LOW | Total | Producer's | 95% Conference |
| REFERENCE MAP | EXTREME | 36 | 11 | 2 | 2 | 51 | 70.59% | 6.38% |
| | HIGH | 1 | 14 | 4 | 6 | 25 | 56.00% | 9.93% |
| | INTERMEDIATE | 0 | 0 | 7 | 18 | 25 | 28.00% | 8.98% |
| | LOW | 0 | 0 | 1 | 57 | 58 | 98.28% | 1.71% |
| | Total | 37 | 25 | 14 | 83 | 159 | | |
| | User's | 97.30% | 56.00% | 50.00% | 68.67% | | 71.70% | 3.57% |
| | 95% Conference | 2.67% | 9.93% | 13.36% | 5.09% | | 68.13% | 75.27% |

*Table 3 - Confusion Matrix of NDWI Mean*

Figure 36 shows the calculated overall accuracy for all the bands/indices using the differencing approach. Overall, the indices outperformed the Landsat 5 bands and differencing on the mean produced better results than standard deviation. As expected the highest accuracy of 71.70% was obtained using differencing of the NDWI, which enhances the water features and Banda Aceh was heavily flooded after the tsunami causing the difference in pre and post imagery of damaged areas to be considerably higher. The NDVI also produced high accuracy which is a little surprising since NDVI enhances the presence of vegetation and the study area was of urban-built up. This could be due to the fact that forest is the dominant ecosystem in the Sumatra Island where Banda Aceh is located and the change in the 'greenness' in the pre and post image

is significant due to the presence of water from flooding. According to Gao (1996), NDWI is a good indicator for water content and is less sensitive to atmospheric scattering effects than NDVI which may be one reason it slightly out performed NDVI. The NDBI is expected to perform better than the results suggest because its aim is to enhance built-up areas and change should be more evident from comparing pre and post imagery. NDBI takes advantage of the fact that built-up has higher reflectance in MIR than in NIR, but some research has shown that vegetation and turbid waters also have the same characteristics which could be the reason for the lower than expected accuracy. From the visible bands, red-band performed the best as expected with just over 50% accuracy. The red out performed blue and green because it has low reflectance from vegetation and impervious surfaces such as built-up have high reflectance representing the change in built-up area more effectively. The low 50% accuracy is probably associated with the complex landscape of a city where a single band can't reflect only the change information but also noise resulting from other factors. The lowest accuracy of 18.87% belonged to the index that was a result of summation of all the bands. This index was a test to see if including all the bands in one variable will be valuable for damage assessment which wasn't the case.

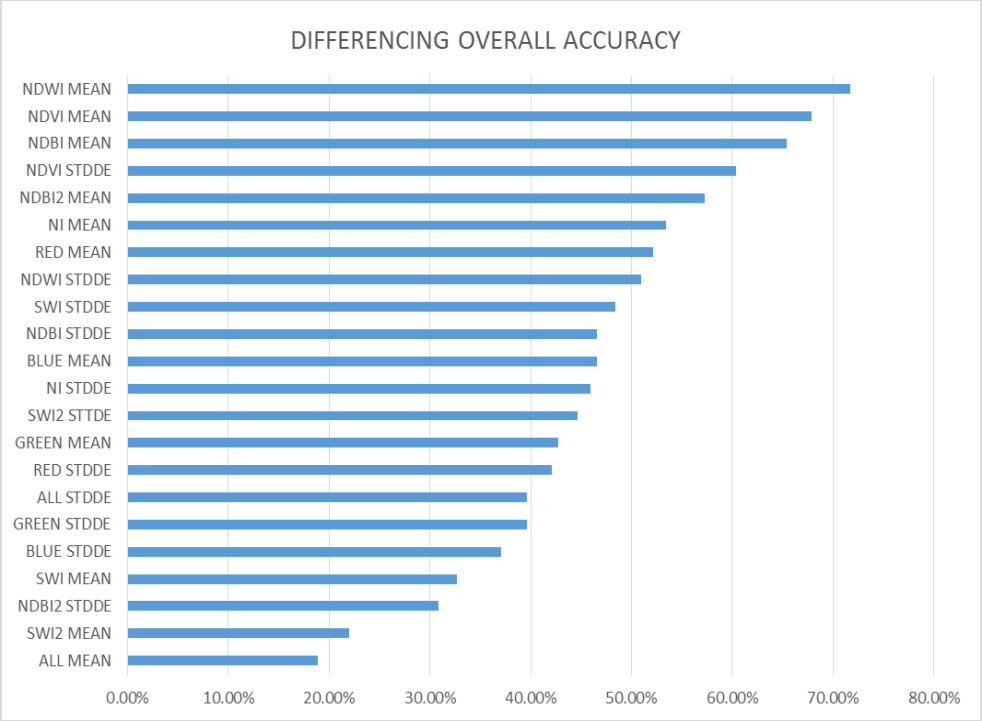


*Figure 36- Image Differencing Overall Accuracies*

Figure 37 shows the calculated overall accuracy for all the bands/indices using the ratioing method. Generally, the indices outperformed the Landsat 5 bands again but the mean accuracies aren't significantly better than the ones obtained by using standard deviation. Equally to the

differencing result, NDWI mean (62.26%) produced the highest accuracy followed by the NDVI mean (59.19%). Unpredictably, NDBI performed lowly compared to the other bands/indices with only 36.38% overall accuracy. Using ratioing, NDBI predicted the extreme and low damage really poorly as the ratio values for extreme damage were the lowest and low damage the highest so the map created had the opposite pattern with extreme damage levels occurring in blocks furthest away from the sea and low damage for blocks bordering/closest to the sea. The red band produced the least accurate map (8.81%) for the same reason as the NDBI. The standard deviation is the measure of how spread out the numbers are and in ratioing the standard deviation seems to have a bigger affect since it produces values closer to the mean values and in some cases outperform the mean with comparing same band/index.

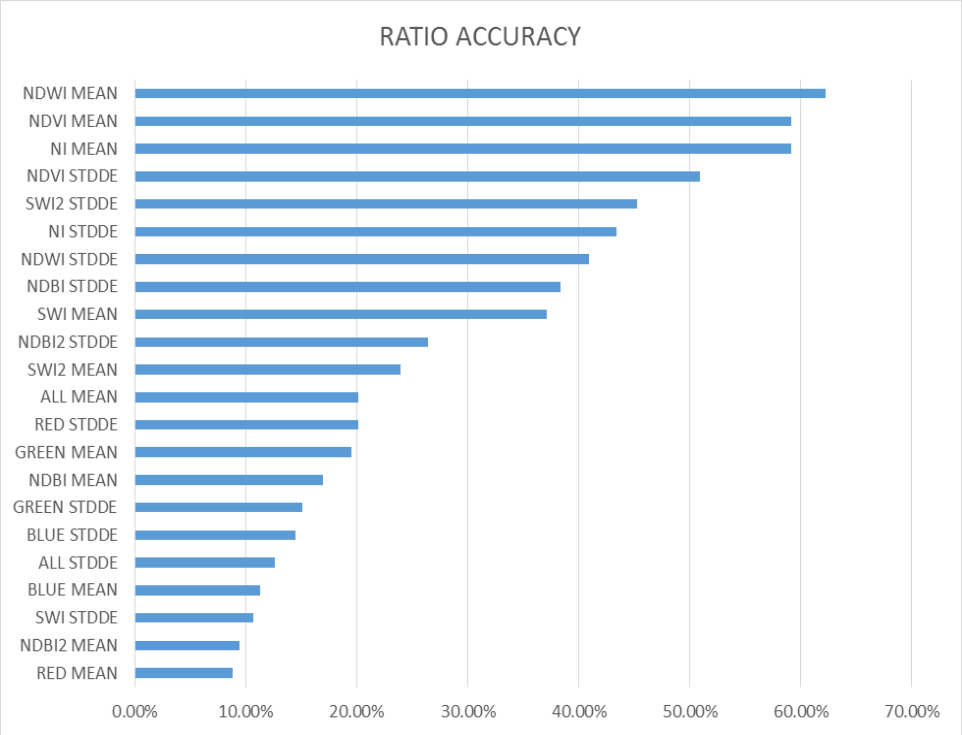


*Figure 37 – Image Ratioing Accuracies*

When comparing differencing accuracy with ratio, it is evident that differencing approach outperformed ratio in almost all bands/indices. Figure 38 shows side by side comparison between the two methods. The variation in the accuracy is surprisingly since in most change detection studies image differencing and ratioing perform similarly in terms of overall accuracy. Singh (1989) achieved 73.16% for differencing and 73.71% for ratioing when detecting change for forest. In almost half the tested bands/indices, differencing had more than

double the accuracy of ratioing. With the use of only Landsat 5 imagery and OSM data, three differencing and one ratioing bands/indices produced accuracy of over 60% which is satisfactory considering the limited resources in terms of data. Using Landsat data, (Macleod 1998) detected change of eelgrass population in New Hampshire. The research concluded that image differencing provided the highest accuracy compared to more complicated methods but with an accuracy of 55%.

The highest overall accuracy in both methods is obtained from the mean NDWI. The mean NDWI (differencing) which produced the highest accuracy is investigated further in order to understand the occurrence of misclassification. Firstly the kappa coefficient is calculated which is another more robust indicator of accuracy as a result of it takes into reason the agreement arising from chance. To define the ideal threshold for change detection images (Fung 1988) evaluated the use of the following accuracy measures: overall, average, combined and Kappa coefficient. The researchers concluded that the Kappa coefficient produced the optimal results because it contemplates all elements of the confusion matrix including the probably associated with chance. The kappa coefficient for the mean NDWI is 59.36% that falls within the range 0.4-0.8, this signifies a mediocre agreement.

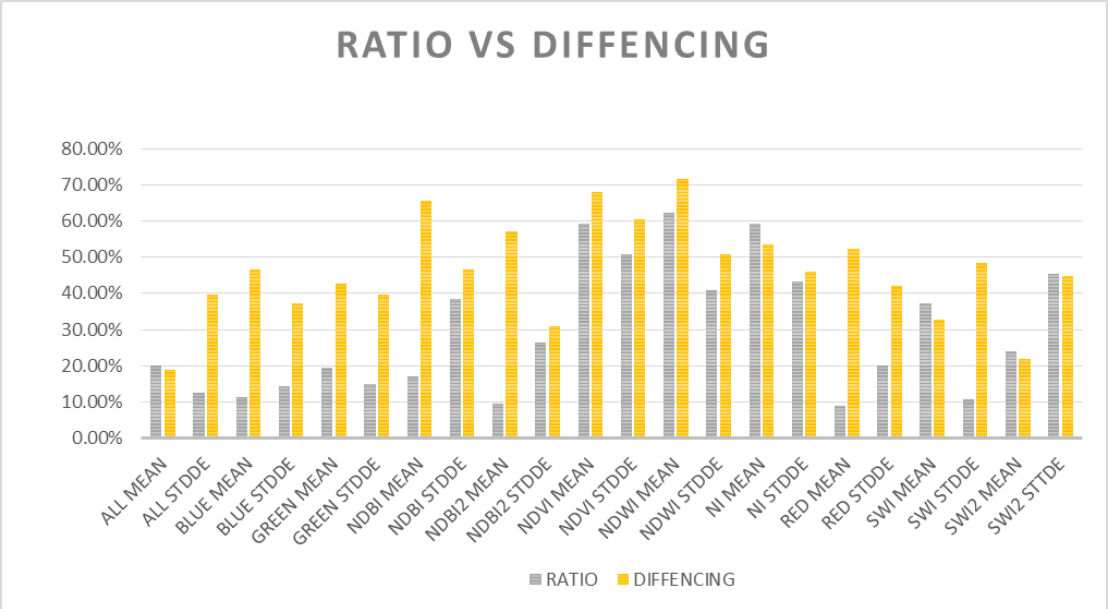


*Figure 38- Ratio Accuracies vs Differencing Accuracies*

In Figure 39, user's and producer's accuracy is compared against the average accuracy to observe where the errors associated with commission and omission occur. For NDWI, the Extreme and Low classes have the same or higher than the average accuracy whereas the high

and intermediate class are both more than 15% below the average accuracy. Most of the confusion between classes happen in the high and intermediate class. Since the main goal of the research is to identify areas most affected by the disaster, and the medium classes cause the most confusion, it is decided to test only using two classes; extreme and low. During a natural disaster, the two most important attributes for emergency response regarding damage are; the most damaged areas to prioritize relief efforts and nearest safe havens to set up temporary housing, clinics, food stations and other emergency services. For the research scope it seems sensible to ignore the blocks associated with the middle classes and only focus on the extremes. Eliminating the blocks associated with the middle classes and only evaluating the extreme and low class will reduce the total blocks from 159 to 109. Predictably, the overall accuracy increased to 85.32% with the area occupied between the classes being a buffer an area of mixed damage. The kappa coefficient also improved to 75.61%. It is therefore evident that having only two damage levels greatly improves the accuracy of NDWI.

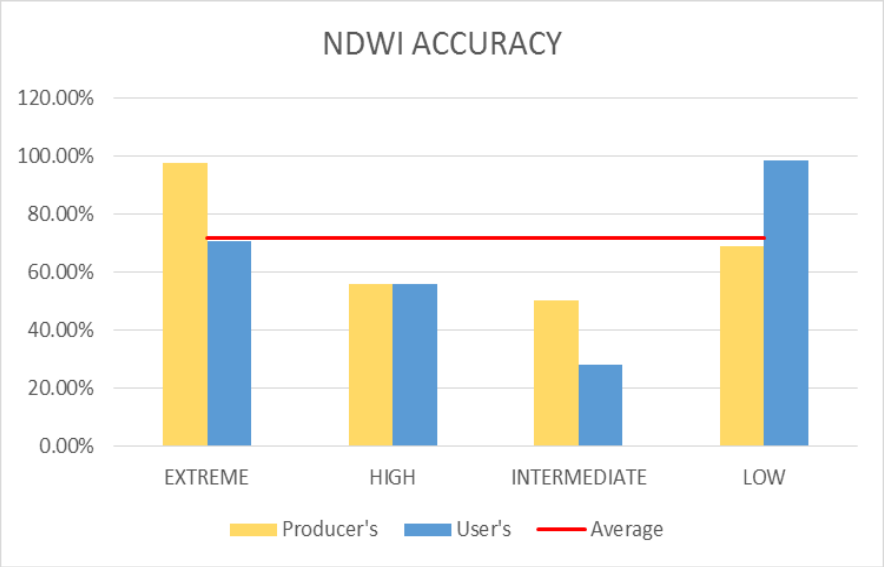


*Figure 39- NDWI Mean, User's, Producer's Accuracies for All Damage Levels*

Figure 40 shows the overall accuracy verses the extreme and low accuracy for all bands/indices. Most of the bands/indices have higher accuracies for extreme and low than the average, indicating that the two class approach will greatly improve the accuracy. It is evident that reducing to two classes will increase the overall accuracy by at least 10% for most of the bands/indices.

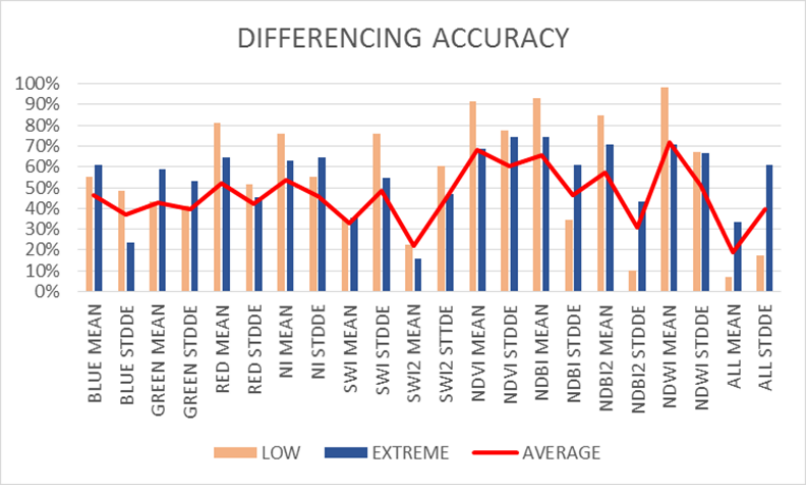


*Figure 40- Overall accuracy vs Extreme and Low Damage for All*

### *5.2.3 Pixel Based Map*

A simple pixel by pixel differencing of NDWI is conducted using the raw pre and post disaster Landsat imagery. The difference values are reclassified into four groups, which corresponds to the four damage levels. Figure 41 shows the resulting map of the displaying damage levels based on pixel by pixel differencing. The rigid map, visually suffers from the "salt and pepper" effect at this scale with many areas inconclusive to which damage level it belongs to due to the variation of damage levels within a proximity.

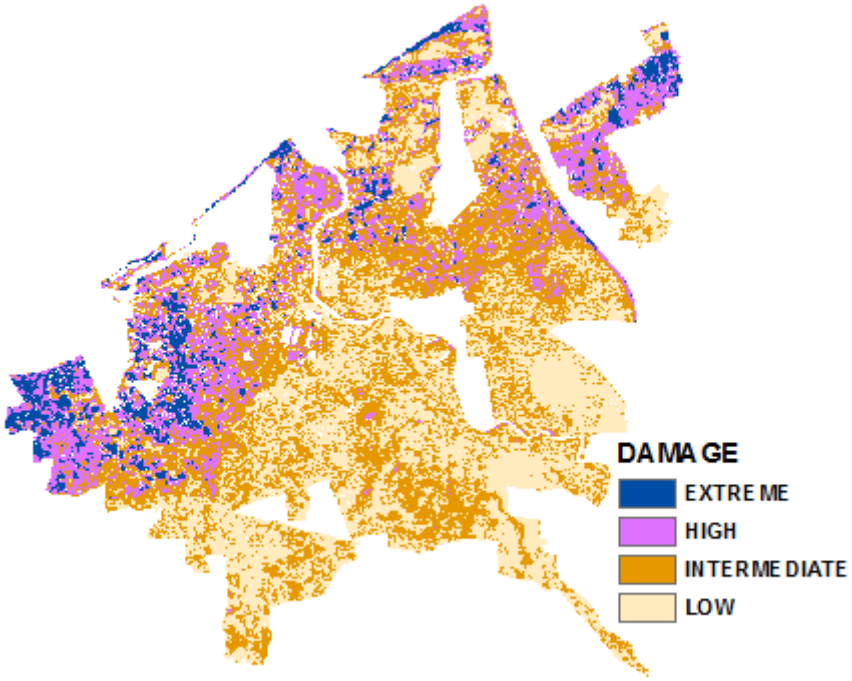


*Figure 41- Damage Map Derived from Pixel by Pixel Differencing*

The pixel NDWI map is then compared to the reference map to evaluate the accuracy. Figure 42 shows a binary map of rightly or wrongly classified pixel compared to the reference map. NDWI map produced an overall accuracy of 42.90% where 31,460 pixels were classified correctly and 41,867 pixels incorrectly seen in Figure 42 (left). Figure 42 (right) illustrates the damage levels of the reference map which is used to evaluate the map created by pixel change detection. Overall pattern for the low damage seems satisfactory but for the extreme damage, the whole northern and north-eastern part are wrongly classified, which can be consequential in terms of allocating emergency services to the most vulnerable areas. With an overall accuracy of 42.90%, it's significantly below the accuracies obtained by using blocks instead of pixels. Not only are the accuracies higher but it's also more visually pleasing with a "cleaner" look that will help emergency response teams, decision makers and other non-GIS users make the right decision regarding the allocation of supplies and resources during a disaster.

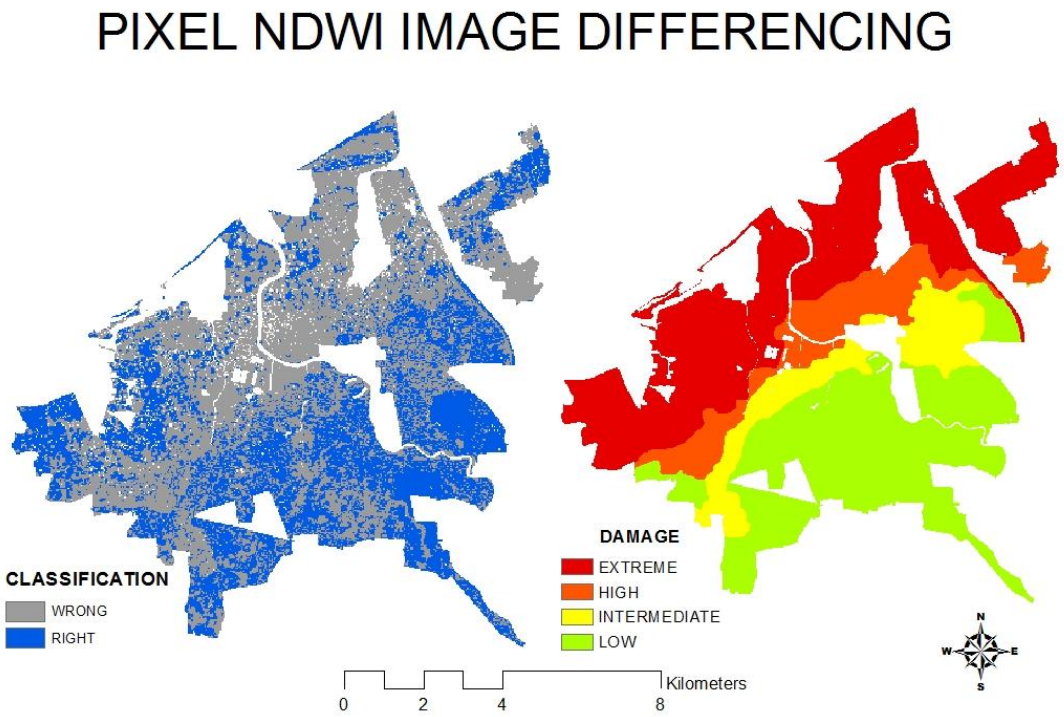


*Figure 42- Pixel Classification Result*

## 5.3 Final Map

Figure 43 illustrates the damage map produced from image differencing of NDWI mean. This combination produced the disaster map with the highest accuracy of 71.70%. The damage map follows the overall pattern of the reference map with the highest damage occurring in areas around the coast and decreasing when regressing from the coast inland. The rapidly generated map provides a clear, easy to interpret "birds-eye view" of the affected area to efficiently and effectively allocate emergency efforts within a short time frame. The time from raw satellite data to damage maps improved to a few hours from the three days it took SERTIT (reference map) which can be immensely beneficial in terms of emergency response efforts. Due to the already defined tools, non-GIS personnel can easily implement the semi-automatic workflow to create damage assessment maps as it requires minimal GIS knowledge.

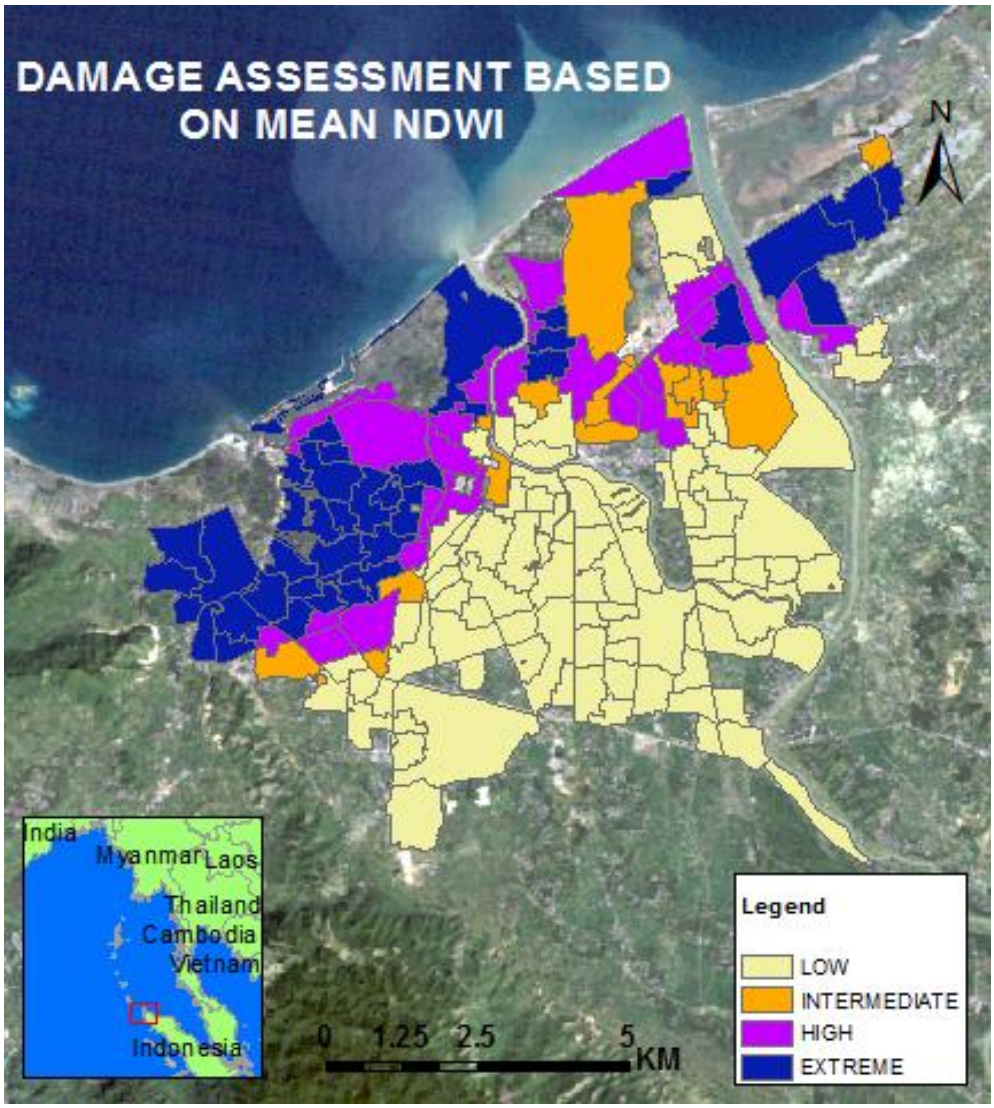


*Figure 43- Final Damage Map*

## 5.4 Most Suitable Temporary Living Sites

The most suitable temporary living sites are selected using MCDA. MCDA selected 14 suitable sites from a possible 114 locations around Banda Aceh (Figure 44). To determine the best locations for temporary housing centres after the Isfahan earthquake in Iran, Naderi (2015) produced desirable lands and integrated local parameters to propose five temporary housing sites which produced an accuracy of 73.3%. Although quantitative analysis can't be applied due to the lack of reference data, visual analysis shows that the proposed temporary living sites correlate well with the UN temporary living center map. The simple method of using four factors and their corresponding derived weights created a meaningful result in finding suitable temporary living sites. The 14 temporary housing sites are located in the southern outskirts of Banda Aceh which is similar to the pattern seen in the UN map.

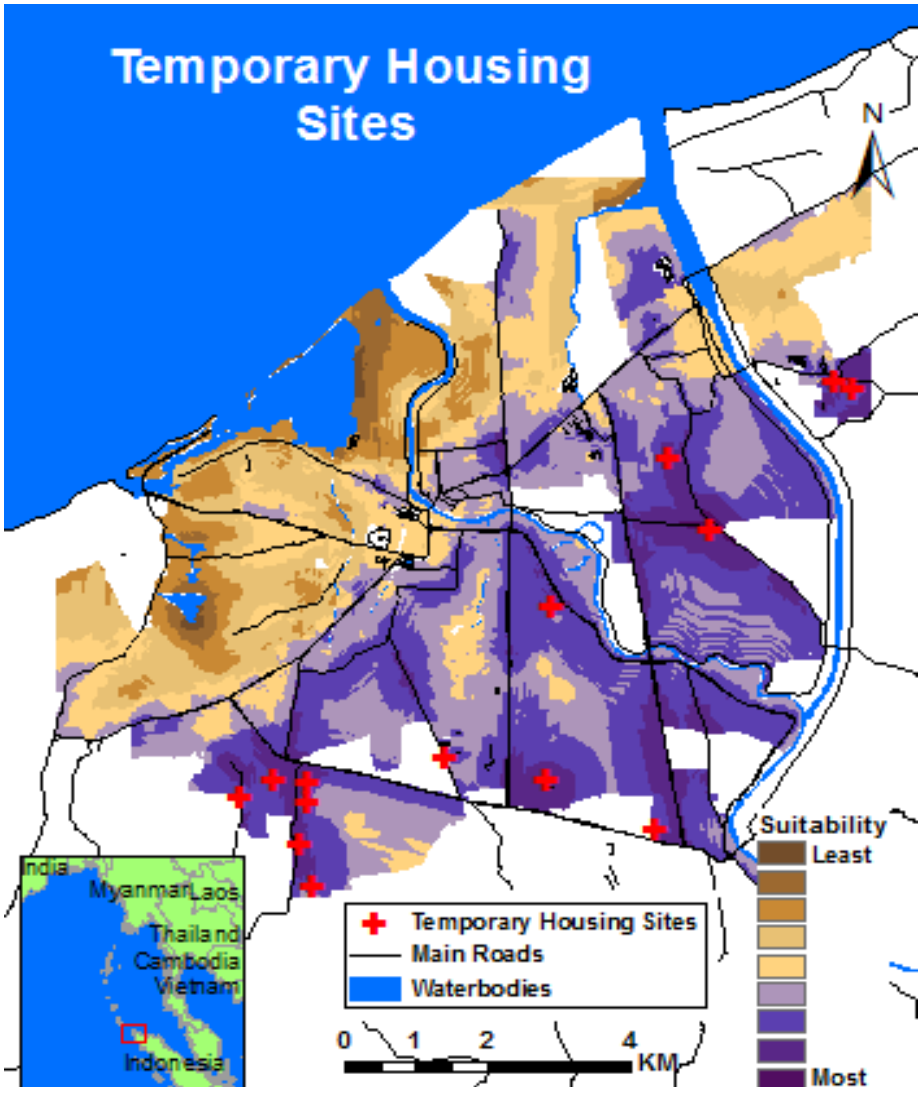


*Figure 44- Temporary Housing Sites Map*

## 5.5 Online Map

Due to the international charter for disaster management's initiative to distribute, share and easily update disaster products, the final disaster map and temporary living centres sites are published online. Publishing the maps on ArcMap Server makes the products remotely accessible from anywhere in the world. The interactive map can easily be updated with new layers of analysis and offers various basemaps to better interpret the most affected areas. The zoom capability coupled with the ease of switching analysis layers can be beneficial in examining the damage taking in multiple factors. The interactive map provides an easily understandable product which can help non-GIS users such as decision makers to maximize the intake of the intended information of the product in order take the appropriate decisions regarding emergency services. Some snapshots of the online map can be seen in Figure 45 and the interactive online map can be found at http://arcg.is/21kGFIr.


*Figure 45 – Online Damage Map (top left), Differencing Change Detection Values (top right) and Close-up of Selected Temporary Housing Site (bottom)*

# 6 CONCLUSION

The integrated global observation strategy's ongoing research and advancement in integrating satellite data from a wide eletromagnetic spectrum with ground in situ measurements has added to the time series dataset of Earth events. This new initiative will help the disaster assessment community better predict, visualize and manage natural disaster events (Tralli 2005). One of the major shortcomings of the International Charter is focus on providing primary raw satellite imagery rather than disaster assessment maps (USDE 1996).

With that in mind, a new semi-automated workflow was successfully created using ArcMap's modelbuilder and python capabilities as well as FME's visual scripting to quantify damage into four levels. The study area was divided into city blocks using the road network and then zonal statistics was applied on all six bands of Landsat 5 (except thermal) and the following indices; NDVI, NDBI and NDWI to detect for change on the city blocks. This hybrid approach took advantage of the simplicity of applying pixel change detection techniques on fixed objects (blocks) to assess for damage. Overall, 44 maps were created using block mean and standard deviation statistics and evaluated against a damage reference map created by SERTIT. Image differencing out performed image ratioing method in almost all bands/indices. The image differencing of NDWI mean produced the highest overall accuracy of 71.70% with four classes and 85.32% with only using two classes. The semi-automatic workflow produced damage maps within a few hours which is a big improvement from the three days it took SERTIT. Although the workflow produced reasonable results within a short time frame, the workflow should be applied to other areas affected by various types of natural disasters to better substantiate the robustness of the workflow. When time is of essence with limited resources and GIS expertise on the field, the semi-automated method introduced in this report is a valuable solution in producing rapid damage maps within a short time.

MCDA was utilized using four factors to select the most suitable locations for temporary living centers. Proximity to water, proximity to roads, building size and the damage map were used using weighted linear combination to predict the most suitable locations. Although no quantitative accuracy measures were applied due to the lack of reference data, the selected sites were visually compared against a UN map of temporary living sites after the 2004 tsunami. The 14 selected sites correlated well when compared to the UN map, with a general trend of temporary living centers around the southern and eastern outskirts of Banda Aceh.

The study was successful in providing a semi-automated workflow in assessing damage for areas stricken by a natural disaster, but further improvement can be made. For future high-resolution mapping of disaster assessment, easily available imagery such as Landsat are not accurate enough, so aerial photographs have to be integrated to acquire infrastructure margins for better in-depth damage analysis. Global gazetteers such as GEOnet can be incorporated to add labeling information for natural and built-up features. For better estimation of the number of people affected by a disaster, population density data from Land-Scan dataset can be incorporated. The use of contour lines to add topographic representation can be derived from DEM data joined with GLOBE 30 data (Voigt 2007). The integration of crowdsourcing and social media data with damage maps can add valuable information in determining areas most heavily hit. Tweets, tagged images and other sources of crowdsourcing data can help save lives by indicating areas most affect by a disaster and filter the overflow of information coming in following a disaster. The downside to adding multiple layers in change detection analysis is the large number of factors in the analysis, which makes it more difficult to assess the accuracy and determine the contribution of each factor to the overall error.

Even though image differencing and image ratioing are among the two most widely used and most robust pixel change detection methods (Singh 1989), all digital change detection methods suffer from the effects of spectral, spatial, temporal and thematic limitations. The qualitative or quantitative estimates are greatly influenced by the change detection method used (Colwell 1981). The selection of the change detection method to be implemented in the future should be of substantial importance due to the fact that different methods will produce different results when testing in the same environment.

# 7 BIBLIOGRAPHY


(ISDR), UN/International Strategy for Disaster Reduction. 2004. *Terminology of disaster risk reduction.* Accessed November 13, 2015. http://www.unisdr.org/eng/library/lib-terminology-eng%20home.htm.

Allenbach, Bernard, Remi Andreoli, Stephanie Battiston, Claude Bestault, Stephen Clandillon, J-B. Henry, C. Meyer, Nadine Tholey, H. Yesou, and Paul De Fraipont. 2005. "Rapid eo disaster mapping service: Added value, feedback and perspectives after 4 years of charter actions." *In Geoscience and Remote Sensing Symposium, 2005. IGARSS'05. Proceedings* 4373-4378.

Bitelli, G., R. Camassi, L. Gusella, and A. Mongnol. 2014. "Image change detection on urban area: the earthquake case." *In XXth ISPRS Congress* 692.

Blaschke, T., S. Lang, E. Lorup, J. Strobl, and P. Zeil. 2000. "Object-oriented image processing in an integrated GIS/remote sensing environment and perspectives for environmental applications." *Environmental Information for Planning, Politics, and the Public vol. 2* 555-570.

Blundell, J.S. and D.W. Opitz. 2006. *Object recognition and feature extraction from imagery: the Feature Analyst® approach.* July 4. Accessed November 10, 2016. http://www.commission4.isprs.org/obia06/papers.htm .

Bovolo, Francesca, and Lorenzo Bruzzone. 2007. "A split-based approach to unsupervised change detection in large-size multitemporal images: Application to tsunami-damage assessment." *Geoscience and Remote Sensing, IEEE Transactions on 45* 1658-1670.

Campagnolo, M.L. and J.O. Cerdeira. 2007. "Contextual classification of remotely sensed images with integer linear programming." *Proceedings of CompIMAGE-Computational Modeling of Objects Represented in Images: Fundamentals, Methods, and Applications* 123-128.

Carrara, Antonini, Fausto Guzzetti, Mauro Cardinali, and P. Reichenbach. 1999. "Use of GIS technology in the prediction and monitoring of landslide hazard." *Natural hazards 20* 117-135.

Carver, Stephen J. 1991. "Integrating multi-criteria evaluation with geographical information systems." *International Journal of Geographical Information System 5* 321-339.

CEOS. 2002. *The use of earth observation satellites for hazard support: Assessments and scenarios. Final report of the CEOS Disaster Management Support Group.* Accessed November 16, 2015. http://www.ceos.org/pages/DMSG/pdf/CEOSDMSG.pdf.

Charter, The International. 2000. *Space and Major Disasters.* Accessed November 10, 2015. http://www.disasterscharter.org.

Colwell, John E., and F. P. Weber. 1981. "Forest change detection." *In International Symposium on Remote Sensing of Environment* 839-852.

County, Saint Louis. n.d. *The Four Phases of Emergency Management.* Accessed November 14, 2015. http://www.stlouisco.com/lawandpublicsafety/emergencymanagement/thefivephasesofemergencymanagement.

Cutter, Susan L. 2003. "GI science, disasters, and emergency management." *Transactions in GIS 7* 439-446.

De Jong, S.M., T. Hornstra, and H. Maas. 2001. "An integrated spatial and spectral approach to the classification of Mediterranean land cover types: the SSC method." *International Journal of Applied Earth Observation and Geoinformation* 176-183.

Dehvari, A., and R. J. Heck. 2009. "Comparison of object-based and pixel based infrared airborne image classification methods using DEM thematic layer." *Journal of Geography and Regional Planning 2* 86-96.

Eastman, J. Ronald, Weigen Jin, P. A. K. Keym, and James Toledano. 1995. "Raster procedures for multi-creteria/multi-objective decisions." *Photogrammetric Engineering and Remote Sensing 61* 539-547.

Economic, United Nations. Dept. of. 2001. *World Urbanization Prospects: The 1999 Revision (Vol. 194).* United Nations Publications.

Eguchi, Ronald T., C. K. Huyck, Beverley J. Adams, Babak Mansouri, Bijan Houshmand, and Masanobu Shinozuka. 2001. "Resilient disaster response: using remote sensing technologies for post-earthquake damage detection." *Earthquake Engineering to Extreme Events (MCEER).*

Enderle, D, and R.C. Weih, Jr. 2005. " Integrating supervised and unsupervised classification methods to develop a more accurate land cover classification." *Journal of the Arkansas Academy of Science* 65-73.

Firl, Grant J., and Lane Carter. 2011. "Lesson 10: Calculating Vegetation Indices from Landsat 5 TM and Landsat 7 ETM+ Data."

Fitzpatrick, Daniel. 2010. "Land and Natural Disasters: Guidance for Practitioners." *LAND AND NATURAL DISASTERS: GUIDANCE FOR PRACTITIONERS, United Nations Human Settlements Programme.*

Fraser R.H., A. Abuelgasim, and R. Latifovic. 2005. "A method for detecting large-scale forest cover change using coarse spatial resolution imagery." *Remote Sensing of Environment* 414-427.

Fung, Tunf, and Ellsworth LeDrew. 1988. "The determination of optimal threshold levels for change detection using various accuracy indices." *Photogrammetric Engineering and Remote Sensing 54* 1449-1454.

G. Bitelli, R. Camassi b, L. Gusella, A. Mognol. 2001. *IMAGE CHANGE DETECTION ON URBAN AREA: THE EARTHQUAKE CASE.* Research Project, Bologna: University of Bologna.

Gao, B.C. 1996. "NDWI—a normalized difference water index for remote sensing of vegetation liquid water from space." *Remote Sensing of Environment* 257–266.

GeoHazards, I. G. O. S. 2004. *GEOHAZARDS theme report: For the Monitoring of our Environment from Space and from Earth.* European Spae Agency publicatiom.

Gitas I.Z., G. Mitri, and G. Ventura. 2004. "Object-based image classification for burned area mapping of Creus Cape, Spain, using NOAA-AVHRR imagery." *Remote Sensing of Environment* 409-413.

Hasegawa, H., Aoki, H., Yamazaki, F., Matsuoka, M. & Sekimoto, I. 2000. "Automated detection of damaged buildings using aerial HDTV images." *Proceedings of the IEEE 2000 International Geoscience and.*

Higgs, Gary. 2006. "Integrating multi-criteria techniques with geographical information systems in waste facility location to enhance public participation." *Waste management & research 24* 105-117.

Jackson, Ray D., and Alfredo R. Huete. 1991. "Interpreting vegetation indices." *Preventive Veterinary Medicine 11* 185-200.

Keeney, R. L., and Raiffa, H. 1976. "Decisions with Multiple Objectives: Preferences and Value Trade-off."

Keller, A. Z., and A. F. Al-Madhari. 1996. "Risk management and disasters." *Disaster Prevention and Management: An International Journal 5* 19-22.

Koc-San, D., B. T. San, V. Bakis, M. Helvaci, and Z. Eker. 2013. "Multi-Criteria Decision Analysis integrated with GIS and remote sensing for astronomical observatory site selection in Antalya province, Turkey." *Advances in Space Research 52* 39-51.

Kraemer, Helena C. 1982. "Kappa coefficient." *Wiley StatsRef: Statistics Reference Online.*

Lindsay, Bruce R. 2012. *Federal Emergency Management: A Brief Introduction.* Analyst in American National Goverment.

Mabin, Vicky, and Michael Beattie. 1999. "A Practical Guide to Multi-Criteria Decision Analysis: A Workbook Companion to V• I• S• A." *teaching monograph 4.*

Macleod, Robb D., and Russell G. Congalton. 1998. "A quantitative comparison of change-detection algorithms for monitoring eelgrass from remotely sensed data." *Photogrammetric engineering and remote sensing 64* 207-216.

Masek, J. G., F. E. Lindsay, and S. N. Goward. 2000. "Dynamics of urban growth in the Washington DC metropolitan area, 1973-1996, from Landsat observations." *International Journal of Remote Sensing 21* 3473-3486.

Matsumaru, Ryo, Kozo Nagami, and Kimio Takeya. 2012. "Reconstruction of the Aceh Region following the 2004 Indian Ocean tsunami disaster: A transportation perspective." *IATSS research 36* 11-19.

McFeeters, S.K. 1996. "The use of normalized difference water index (NDWI) in the delineation of open water features." *International Journal of Remote Sensing* 1425–1432.

McRoberts, Ronald E., and Erkki O. Tomppo. 2007. "Remote sensing support for national forest inventories." *Remote Sensing of Environment 110* 412-419.

Mitomi, H., Yamazaki, F. & Matsuoka, M. 2000. "Automated detection of building damage due to recent." *Proceedings of the 21st Asian Conference on Remote Sensing.* 401-406.

Mitomi, H., Yamazaki, F. & Matsuoka, M. 2001. " Development of automated extraction method for building." *Proceedings of the 8th International Conference on.* 8.

Morisette, Jeffrey T., and Siamak Khorram. 2000. "Accuracy assessment curves for satellite-based change detection." *Photogrammetric Engineering and Remote Sensing 66* 875-880.

Naderi, N., and J. Mohammadi. 2015. "Locating Temporary Housing after the Earthquake, Using GIS and AHP Techniques (A Case Study: 15 Districts of Isfahan City)." *Journal of Social Issues & Humanities* 2345-2633.

Navalgund, Ranganath R., V. Jayaraman, and P. S. Roy. 2007. "Remote sensing applications: An overview." *Current Science 93* 1747-1766.

NDR, U.S. National Committee for the Decade for Natural Disaster Reduction. 1991. *A Safer Future: Reducing the Impacts of Natural Disasters.* Washington: The National Academies Press.

Nijkamp, P. 1980. "Environmental Policy Analysis:Operational Methods and Models."

Openshaw, S., Carver, S. J., and Fernie, J. 1989. "Britain's Nuclear Waste: Safety and Siting."

Peduzzi, Pascal, and H. Dao C. Herold. 2005. "Mapping disastrous natural hazards using global datasets." *Natural Hazards 35* 265-289.

Rejaie, Ali, and Masanobu Shinozuka. 2004. "Reconnaissance of Golcuk 1999 earthquake damage using satellite images." *Journal of Aerospace Engineering 17* 20-25.

Safety, Canada Public. 2010. *Emergency Management Planning Guide.* Accessed November 13, 2015. http://www.publicsafety.gc.ca/cnt/rsrcs/pblctns/mrgnc-mngmnt-pnnng/index-en.aspx.

Singh, Ashbindu. 1989. "Review article digital change detection techniques using remotely-sensed data." *International journal of remote sensing 10* 989-1003.

Song, Conghe, Curtis E. Woodcock, Karen C. Seto, Mary Pax Lenney, and Scott A. Macomber. 2001. "Classification and change detection using Landsat TM data: when and how to correct atmospheric effects?" *Remote sensing of Environment 75* 230-244.

Tayyebia, A. H., M. R. Delavara, A. Tayyebia, and M. Golobi. 2010. "Combining multi criteria decision making and Dempster Shafer theory for landfill site selection." *International Archives of the Photogrammetry, Remote Sensing and Spatial Information Science.*

Tralli, David M., Ronald G. Blom, Victor Zlotnicki, Andrea Donnellan, and Diane L. Evans. 2005. "Satellite remote sensing of earthquake, volcano, flood, landslide and coastal inundation hazards." *ISPRS Journal of Photogrammetry and Remote Sensing 59* 185-198.

UNDP, HDR. 2004. *Reducing Disaster Risk: A Challenge for Development–A Global Report.* New York: UNDP.

USAID/OAS. 1997. "Caribbean Disaster Mitigation Project." Sustainable Development and Environment, Washington.

USDE, Unit of Sustainable Development Environment. 1996. *Planning to Mitigate the Impacts of Natural Hazards in the Caribbean.* Washington: USAID/OAS.

USGS, National Earthquake Information Center. 2010. "USGS Energy and Broadband Solution." *US Geological Survey.*

Voigt, Stefan, Thomas Kemper, Torsten Riedlinger, Ralph Kiefl, Klaas Scholte, and Harald Mehl. 2007. "Satellite image analysis for disaster and crisis-management support." *Geoscience and Remote Sensing, IEEE Transactions on 45* 1520-1528.

Wang, Jiang-Jiang, You-Yin Jing, Chun-Fa Zhang, and Jun-Hong Zhao. 2009. "Review on multi-criteria decision analysis aid in sustainable energy decision-making." *Renewable and Sustainable Energy Reviews 13* 2263-2278.

Webb, Elizabeth E., and Susan EH Sakimoto. 2009. "Re-mapping the 2004 Boxing Day Tsunami Inundation in the Banda Aceh Region with Attention to Probable Sea Level Rise."

Weih Jr, Robert C., and Norman D. Riggan Jr. 2010. "Object-based classification vs. pixel-based classification: comparative importance of multi-resolution imagery." *Proceedings of GEOBIA 2010: Geographic Object-Based Image Analysis 38.*

Willhauck, G., T. Schneider, R. De Kok, and U. Ammer. 2000. "Comparison of object oriented classification techniques and standard image analysis for the use of change detection between SPOT multispectral satellite images and aerial photos." *In Proceedings of XIX ISPRS congress* 35-42.

Xian, G. and M. Crane. 2005. "Assessments of urban growth in the Tampa Bay watershed using remote sensing data." *Remote Sensing of Environment* 203-215.

Xu, Hanqi u. 2007. "Extraction of urban built-up land features from Landsat imagery using a thematicoriented index combination technique." *Photogrammetric Engineering & Remote Sensing 73* 1381-1391.

Xu, Han-qiu. 2002. "An assessment of land use changes in Fuqing county of China using remote sensing technology." *Chinese Geographical Science 12* 126-135.

Xu, Hanqiu. 2006. "Modification of normalised difference water index (NDWI) to enhanceopen water features in remotely sensed imagery." *International Journal of Remote Sensing* 3025-3033.

Yamazaki, Fumio. 2001. "Applications of remote sensing and GIS for damage assessment." *Structural Safety and Reliability* 1-12.

YAO, Sico Stevens A. 2004. "Visual Learning Systems, Inc."

Z. Cakir, J.B. Chabalier, R. Armijo, B. Meyer, A. Barka, G. Peltzer. 2003. "Coseismic and early post-seismic slip associated with the 1999 Izmit earthquake (Turkey), from SAR interferometry and tectonic field observations." *Geophysical Journal International* 93-110.

Zha, Yong, Jay Gao, and Shaoxiang Ni. 2003. "Use of normalized difference built-up index in automatically mapping urban areas from TM imagery." *International Journal of Remote Sensing 24* 583-594.

Zhang, Q., J. Wang, X. Peng, P. Gong, and P. Shi. 2002. "Urban built-up land change detection with road density and spectral information from multi-temporal Landsat TM data." *International Journal of Remote Sensing 23* 3057-3078.

# 8 APPENDICES

## 8.1 APPENDIX 1 – Confusion Matrices

### *8.1.1 Image Differencing*

BLUE MEAN

| | EXTREME | HIGH | INTERMEDIATE | LOW | | Producer's | |
|---|---|---|---|---|---|---|---|
| EXTREME | 31 | 15 | 4 | 1 | 51 | 60.78% | 6.84% |
| HIGH | 2 | 7 | 4 | 12 | 25 | 28.00% | 8.98% |
| INTERMEDIATE | 0 | 1 | 4 | 20 | 25 | 16.00% | 7.33% |
| LOW | 2 | 13 | 11 | 32 | 58 | 55.17% | 6.53% |
| | 35 | 36 | 23 | 65 | 159 | | |
| User's | 88.57% | 19.44% | 17.39% | 49.23% | | 46.54% | 3.96% |
| | 5.38% | 6.60% | 7.90% | 6.20% | | 42.59% | 50.50% |

BLUE STDDE

| | EXTREME | HIGH | INTERMEDIATE | LOW | | Producer's | |
|---|---|---|---|---|---|---|---|
| EXTREME | 12 | 14 | 4 | 21 | 51 | 23.53% | 5.94% |
| HIGH | 5 | 13 | 5 | 2 | 25 | 52.00% | 9.99% |
| INTERMEDIATE | | 11 | 6 | 8 | 25 | 24.00% | 8.54% |
| LOW | 5 | 20 | 5 | 28 | 58 | 48.28% | 6.56% |
| | 22 | 58 | 20 | 59 | 159 | | |
| User's | 54.55% | 22.41% | 30.00% | 47.46% | | 37.11% | 3.83% |
| | 10.62% | 5.48% | 10.25% | 6.50% | | 33.28% | 40.94% |

GREEN MEAN

| | EXTREME | HIGH | INTERMEDIATE | LOW | | Producer's | |
|---|---|---|---|---|---|---|---|
| EXTREME | 30 | 14 | 4 | 3 | 51 | 58.82% | 6.89% |
| HIGH | 2 | 7 | 6 | 10 | 25 | 28.00% | 8.98% |
| INTERMEDIATE | | 1 | 6 | 18 | 25 | 24.00% | 8.54% |
| LOW | 3 | 20 | 10 | 25 | 58 | 43.10% | 6.50% |
| | 35 | 42 | 26 | 56 | 159 | | |
| User's | 85.71% | 16.67% | 23.08% | 44.64% | | 42.77% | 3.92% |
| | 5.91% | 5.75% | 8.26% | 6.64% | | 38.84% | 46.69% |

GREEN STDDE

| | EXTREME | HIGH | INTERMEDIATE | LOW | | Producer's | |
|---|---|---|---|---|---|---|---|
| EXTREME | 27 | 9 | 2 | 13 | 51 | 52.94% | 6.99% |
| HIGH | 5 | 11 | 1 | 8 | 25 | 44.00% | 9.93% |
| INTERMEDIATE | 1 | 13 | 1 | 10 | 25 | 4.00% | 3.92% |
| LOW | 13 | 18 | 3 | 24 | 58 | 41.38% | 6.47% |
| | 46 | 51 | 7 | 55 | 159 | | |
| User's | 58.70% | 21.57% | 14.29% | 43.64% | | 39.62% | 3.88% |
| | 7.26% | 5.76% | 13.23% | 6.69% | | 35.74% | 43.50% |

RED MEAN

| | EXTREME | HIGH | INTERMEDIATE | LOW | | Producer's | |
|---|---|---|---|---|---|---|---|
| EXTREME | 33 | 8 | 5 | 5 | 51 | 64.71% | 6.69% |
| HIGH | 2 | 1 | 7 | 15 | 25 | 4.00% | 3.92% |
| INTERMEDIATE | | | 2 | 23 | 25 | 8.00% | 5.43% |
| LOW | 1 | 5 | 5 | 47 | 58 | 81.03% | 5.15% |
| | 36 | 14 | 19 | 90 | 159 | | |
| User's | 91.67% | 7.14% | 10.53% | 52.22% | | 52.20% | 3.96% |
| | 4.61% | 6.88% | 7.04% | 5.27% | | 48.24% | 56.16% |

RED STDDE

| | EXTREME | HIGH | INTERMEDIATE | LOW | | Producer's | |
|---|---|---|---|---|---|---|---|
| EXTREME | 23 | 8 | 1 | 19 | 51 | 45.10% | 6.97% |
| HIGH | 5 | 8 | 4 | 8 | 25 | 32.00% | 9.33% |
| INTERMEDIATE | 1 | 7 | 6 | 11 | 25 | 24.00% | 8.54% |
| LOW | 9 | 13 | 6 | 30 | 58 | 51.72% | 6.56% |
| | 38 | 36 | 17 | 68 | 159 | | |
| User's | 60.53% | 22.22% | 35.29% | 44.12% | | 42.14% | 3.92% |
| | 7.93% | 6.93% | 11.59% | 6.02% | | 38.22% | 46.05% |

NI MEAN

| | EXTREME | HIGH | INTERMEDIATE | LOW | | Producer's | |
|---|---|---|---|---|---|---|---|
| EXTREME | 32 | 6 | 9 | 4 | 51 | 62.75% | 6.77% |
| HIGH | 10 | 5 | 3 | 7 | 25 | 20.00% | 8.00% |
| INTERMEDIATE | | 3 | 4 | 18 | 25 | 16.00% | 7.33% |
| LOW | | 5 | 9 | 44 | 58 | 75.86% | 5.62% |
| | 42 | 19 | 25 | 73 | 159 | | |
| User's | 76.19% | 26.32% | 16.00% | 60.27% | | 53.46% | 3.96% |
| | 6.57% | 10.10% | 7.33% | 5.73% | | 49.50% | 57.41% |

NI STDDE

| | EXTREME | HIGH | INTERMEDIATE | LOW | | Producer's | |
|---|---|---|---|---|---|---|---|
| EXTREME | 33 | 8 | 1 | 9 | 51 | 64.71% | 6.69% |
| HIGH | 10 | 5 | 1 | 9 | 25 | 20.00% | 8.00% |
| INTERMEDIATE | 4 | 2 | 3 | 16 | 25 | 12.00% | 6.50% |
| LOW | 4 | 9 | 13 | 32 | 58 | 55.17% | 6.53% |
| | 51 | 24 | 18 | 66 | 159 | | |
| User's | 64.71% | 20.83% | 16.67% | 48.48% | | 45.91% | 3.95% |
| | 6.69% | 8.29% | 8.78% | 6.15% | | 41.96% | 49.86% |

SWI MEAN

| | EXTREME | HIGH | INTERMEDIATE | LOW | | Producer's | |
|---|---|---|---|---|---|---|---|
| EXTREME | 18 | 16 | 5 | 12 | 51 | 35.29% | 6.69% |
| HIGH | 1 | 10 | 5 | 9 | 25 | 40.00% | 9.80% |
| INTERMEDIATE | | 3 | 4 | 18 | 25 | 16.00% | 7.33% |
| LOW | 6 | 24 | 8 | 20 | 58 | 34.48% | 6.24% |
| | 25 | 53 | 22 | 59 | 159 | | |
| User's | 72.00% | 18.87% | 18.18% | 33.90% | | 32.70% | 3.72% |
| | 8.98% | 5.37% | 8.22% | 6.16% | | 28.98% | 36.42% |

SWI STDDE

| | EXTREME | HIGH | INTERMEDIATE | LOW | | Producer's | |
|---|---|---|---|---|---|---|---|
| EXTREME | 28 | 9 | 3 | 11 | 51 | 54.90% | 6.97% |
| HIGH | 2 | 3 | 5 | 15 | 25 | 12.00% | 6.50% |
| INTERMEDIATE | | 1 | 2 | 22 | 25 | 8.00% | 5.43% |
| LOW | | 6 | 8 | 44 | 58 | 75.86% | 5.62% |
| | 30 | 19 | 18 | 92 | 159 | | |
| User's | 93.33% | 15.79% | 11.11% | 47.83% | | 48.43% | 3.96% |
| | 4.55% | 8.37% | 7.41% | 5.21% | | 44.46% | 52.39% |

SWI2 MEAN

| | EXTREME | HIGH | INTERMEDIATE | LOW | | Producer's | |
|---|---|---|---|---|---|---|---|
| EXTREME | 8 | 8 | 6 | 29 | 51 | 15.69% | 5.09% |
| HIGH | 2 | 4 | 7 | 12 | 25 | 16.00% | 7.33% |
| INTERMEDIATE | 1 | 7 | 10 | 7 | 25 | 40.00% | 9.80% |
| LOW | 1 | 12 | 32 | 13 | 58 | 22.41% | 5.48% |
| | 12 | 31 | 55 | 61 | 159 | | |
| User's | 66.67% | 12.90% | 18.18% | 21.31% | | 22.01% | 3.29% |
| | 13.61% | 6.02% | 5.20% | 5.24% | | 18.73% | 25.30% |

SWI2 STTDE

| | EXTREME | HIGH | INTERMEDIATE | LOW | | Producer's | |
|---|---|---|---|---|---|---|---|
| EXTREME | 24 | 9 | 2 | 16 | 51 | 47.06% | 6.99% |
| HIGH | 9 | 7 | 4 | 5 | 25 | 28.00% | 8.98% |
| INTERMEDIATE | 1 | 10 | 5 | 9 | 25 | 20.00% | 8.00% |
| LOW | 1 | 10 | 12 | 35 | 58 | 60.34% | 6.42% |
| | 35 | 36 | 23 | 65 | 159 | | |
| User's | 68.57% | 19.44% | 21.74% | 53.85% | | 44.65% | 3.94% |
| | 7.85% | 6.60% | 8.60% | 6.18% | | 40.71% | 48.60% |

NDVI MEAN

| | EXTREME | HIGH | INTERMEDIATE | LOW | | Producer's | |
|---|---|---|---|---|---|---|---|
| EXTREME | 35 | 13 | 2 | 1 | 51 | 68.63% | 6.50% |
| HIGH | 1 | 15 | 3 | 6 | 25 | 60.00% | 9.80% |
| INTERMEDIATE | | 2 | 5 | 18 | 25 | 20.00% | 8.00% |
| LOW | | 1 | 4 | 53 | 58 | 91.38% | 3.69% |
| | 36 | 31 | 14 | 78 | 159 | | |
| User's | 97.22% | 48.39% | 35.71% | 67.95% | | 67.92% | 3.70% |
| | 2.74% | 8.98% | 12.81% | 5.28% | | 64.22% | 71.63% |

NDVI STDDE

| | EXTREME | HIGH | INTERMEDIATE | LOW | | Producer's | |
|---|---|---|---|---|---|---|---|
| EXTREME | 38 | 10 | 3 | | 51 | 74.51% | 6.10% |
| HIGH | 3 | 9 | 8 | 5 | 25 | 36.00% | 9.60% |
| INTERMEDIATE | 1 | | 4 | 20 | 25 | 16.00% | 7.33% |
| LOW | | 2 | 11 | 45 | 58 | 77.59% | 5.48% |
| | 42 | 21 | 26 | 70 | 159 | | |
| User's | 90.48% | 42.86% | 15.38% | 64.29% | | 60.38% | 3.88% |
| | 4.53% | 10.80% | 7.08% | 5.73% | | 56.50% | 64.26% |

NDBI MEAN

| | EXTREME | HIGH | INTERMEDIATE | LOW | | Producer's | |
|---|---|---|---|---|---|---|---|
| EXTREME | 38 | 10 | | 3 | 51 | 74.51% | 6.10% |
| HIGH | 7 | 10 | 3 | 5 | 25 | 40.00% | 9.80% |
| INTERMEDIATE | | 5 | 2 | 18 | 25 | 8.00% | 5.43% |
| LOW | | 1 | 3 | 54 | 58 | 93.10% | 3.33% |
| | 45 | 26 | 8 | 80 | 159 | | |
| User's | 84.44% | 38.46% | 25.00% | 67.50% | | 65.41% | 3.77% |
| | 5.40% | 9.54% | 15.31% | 5.24% | | 61.64% | 69.18% |

NDBI STDDE

| | EXTREME | HIGH | INTERMEDIATE | LOW | | Producer's | |
|---|---|---|---|---|---|---|---|
| EXTREME | 31 | 7 | 9 | 4 | 51 | 60.78% | 6.84% |
| HIGH | 8 | 7 | 5 | 5 | 25 | 28.00% | 8.98% |
| INTERMEDIATE | 1 | 1 | 16 | 7 | 25 | 64.00% | 9.60% |
| LOW | 3 | 8 | 27 | 20 | 58 | 34.48% | 6.24% |
| | 43 | 23 | 57 | 36 | 159 | | |
| User's | 72.09% | 30.43% | 28.07% | 55.56% | | 46.54% | 3.96% |
| | 6.84% | 9.59% | 5.95% | 8.28% | | 42.59% | 50.50% |

NDBI2 MEAN

| | EXTREME | HIGH | INTERMEDIATE | LOW | | Producer's | |
|---|---|---|---|---|---|---|---|
| EXTREME | 36 | 8 | 2 | 5 | 51 | 70.59% | 6.38% |
| HIGH | 13 | 5 | | 7 | 25 | 20.00% | 8.00% |
| INTERMEDIATE | 1 | 6 | 1 | 17 | 25 | 4.00% | 3.92% |
| LOW | | 6 | 3 | 49 | 58 | 84.48% | 4.75% |
| | 50 | 25 | 6 | 78 | 159 | | |
| User's | 72.00% | 20.00% | 16.67% | 62.82% | | 57.23% | 3.92% |
| | 6.35% | 8.00% | 15.21% | 5.47% | | 53.31% | 61.16% |

NDBI2 STDDE

| | EXTREME | HIGH | INTERMEDIATE | LOW | | Producer's | |
|---|---|---|---|---|---|---|---|
| EXTREME | 22 | 9 | 15 | 5 | 51 | 43.14% | 6.94% |
| HIGH | 5 | 9 | 9 | 2 | 25 | 36.00% | 9.60% |
| INTERMEDIATE | 2 | 4 | 12 | 7 | 25 | 48.00% | 9.99% |
| LOW | 3 | 11 | 38 | 6 | 58 | 10.34% | 4.00% |
| | 32 | 33 | 74 | 20 | 159 | | |
| User's | 68.75% | 27.27% | 16.22% | 30.00% | | 30.82% | 3.66% |
| | 8.19% | 7.75% | 4.28% | 10.25% | | 27.16% | 34.48% |

NDWI MEAN

| | EXTREME | HIGH | INTERMEDIATE | LOW | | Producer's | |
|---|---|---|---|---|---|---|---|
| EXTREME | 36 | 11 | 2 | 2 | 51 | 70.59% | 6.38% |
| HIGH | 1 | 14 | 4 | 6 | 25 | 56.00% | 9.93% |
| INTERMEDIATE | | | 7 | 18 | 25 | 28.00% | 8.98% |
| LOW | | | 1 | 57 | 58 | 98.28% | 1.71% |
| | 37 | 25 | 14 | 83 | 159 | | |
| User's | 97.30% | 56.00% | 50.00% | 68.67% | | 71.70% | 3.57% |
| | 2.67% | 9.93% | 13.36% | 5.09% | | 68.13% | 75.27% |

NDWI STDDE

| | EXTREME | HIGH | INTERMEDIATE | LOW | | Producer's | |
|---|---|---|---|---|---|---|---|
| EXTREME | 34 | 7 | 3 | 7 | 51 | 66.67% | 6.60% |
| HIGH | 6 | 5 | 5 | 9 | 25 | 20.00% | 8.00% |
| INTERMEDIATE | 1 | | 3 | 21 | 25 | 12.00% | 6.50% |
| LOW | 4 | 6 | 9 | 39 | 58 | 67.24% | 6.16% |
| | 45 | 18 | 20 | 76 | 159 | | |
| User's | 75.56% | 27.78% | 15.00% | 51.32% | | 50.94% | 3.96% |
| | 6.41% | 10.56% | 7.98% | 5.73% | | 46.98% | 54.91% |

ALL MEAN

| | EXTREME | HIGH | INTERMEDIATE | LOW | | Producer's | |
|---|---|---|---|---|---|---|---|
| EXTREME | 17 | 14 | 9 | 11 | 51 | 33.33% | 6.60% |
| HIGH | 1 | 4 | 5 | 15 | 25 | 16.00% | 7.33% |
| INTERMEDIATE | | 15 | 5 | 5 | 25 | 20.00% | 8.00% |
| LOW | 21 | 21 | 12 | 4 | 58 | 6.90% | 3.33% |
| | 39 | 54 | 31 | 35 | 159 | | |
| User's | 43.59% | 7.41% | 16.13% | 11.43% | | 18.87% | 3.10% |
| | 7.94% | 3.56% | 6.61% | 5.38% | | 15.77% | 21.97% |

ALL STDDE

| | EXTREME | HIGH | INTERMEDIATE | LOW | | Producer's | |
|---|---|---|---|---|---|---|---|
| EXTREME | 31 | 10 | 7 | 3 | 51 | 60.78% | 6.84% |
| HIGH | 3 | 9 | 10 | 3 | 25 | 36.00% | 9.60% |
| INTERMEDIATE | | 8 | 13 | 4 | 25 | 52.00% | 9.99% |
| LOW | 2 | 26 | 20 | 10 | 58 | 17.24% | 4.96% |
| | 36 | 53 | 50 | 20 | 159 | | |
| User's | 86.11% | 16.98% | 26.00% | 50.00% | | 39.62% | 3.88% |
| | 5.76% | 5.16% | 6.20% | 11.18% | | 35.74% | 43.50% |

### *8.1.2 Image Ratioing*

BLUE MEAN

| | EXTREME | HIGH | INTERMEDIATE | LOW | | User's | |
|---|---|---|---|---|---|---|---|
| EXTREME | | 2 | 12 | 37 | 51 | 0.00% | 0.00% |
| HIGH | 6 | 6 | 11 | 2 | 25 | 24.00% | 8.54% |
| INTERMEDIATE | 6 | 14 | 5 | | 25 | 20.00% | 8.00% |
| LOW | 13 | 9 | 29 | 7 | 58 | 12.07% | 4.28% |
| | 25 | 31 | 57 | 46 | 159 | | |
| Producer's | 0.00% | 19.35% | 8.77% | 15.22% | | 11.32% | 2.51% |
| | 0.00% | 7.10% | 3.75% | 5.30% | | 8.81% | 13.83% |

BLUE STDDE

| | EXTREME | HIGH | INTERMEDIATE | LOW | | User's | |
|---|---|---|---|---|---|---|---|
| EXTREME | 2 | 6 | 21 | 22 | 51 | 3.92% | 2.72% |
| HIGH | 3 | 7 | 13 | 2 | 25 | 28.00% | 8.98% |
| INTERMEDIATE | | 12 | 11 | 2 | 25 | 44.00% | 9.93% |
| LOW | 3 | 24 | 28 | 3 | 58 | 5.17% | 2.91% |
| | 8 | 49 | 73 | 29 | 159 | | |
| Producer's | 25.00% | 14.29% | 15.07% | 10.34% | | 14.47% | 2.79% |
| | 15.31% | 5.00% | 4.19% | 5.66% | | 11.68% | 17.25% |

GREEN MEAN

| | EXTREME | HIGH | INTERMEDIATE | LOW | | User's | |
|---|---|---|---|---|---|---|---|
| EXTREME | 1 | | 19 | 31 | 51 | 1.96% | 1.94% |
| HIGH | 2 | 5 | 16 | 2 | 25 | 20.00% | 8.00% |
| INTERMEDIATE | | 8 | 17 | | 25 | 68.00% | 9.33% |
| LOW | 4 | 14 | 32 | 8 | 58 | 13.79% | 4.53% |
| | 7 | 27 | 84 | 41 | 159 | | |
| Producer's | 14.29% | 18.52% | 20.24% | 19.51% | | 19.50% | 3.14% |
| | 13.23% | 7.48% | 4.38% | 6.19% | | 16.35% | 22.64% |

GREEN STDDE

| | EXTREME | HIGH | INTERMEDIATE | LOW | | User's | |
|---|---|---|---|---|---|---|---|
| EXTREME | | 8 | 9 | 34 | 51 | 0.00% | 0.00% |
| HIGH | 2 | 7 | 14 | 2 | 25 | 28.00% | 8.98% |
| INTERMEDIATE | | 14 | 7 | 4 | 25 | 28.00% | 8.98% |
| LOW | 3 | 24 | 21 | 10 | 58 | 17.24% | 4.96% |
| | 5 | 53 | 51 | 50 | 159 | | |
| Producer's | 0.00% | 13.21% | 13.73% | 20.00% | | 15.09% | 2.84% |
| | 0.00% | 4.65% | 4.82% | 5.66% | | 12.26% | 17.93% |

RED MEAN

| | EXTREME | HIGH | INTERMEDIATE | LOW | | User's | |
|---|---|---|---|---|---|---|---|
| EXTREME | | 13 | 20 | 18 | 51 | 0.00% | 0.00% |
| HIGH | 10 | 13 | 1 | 1 | 25 | 52.00% | 9.99% |
| INTERMEDIATE | 18 | 7 | | | 25 | 0.00% | 0.00% |
| LOW | 27 | 22 | 8 | 1 | 58 | 1.72% | 1.71% |
| | 55 | 55 | 29 | 20 | 159 | | |
| Producer's | 0.00% | 23.64% | 0.00% | 5.00% | | 8.81% | 2.25% |
| | 0.00% | 5.73% | 0.00% | 4.87% | | 6.56% | 11.05% |

RED STDDE

| | EXTREME | HIGH | INTERMEDIATE | LOW | | User's | |
|---|---|---|---|---|---|---|---|
| EXTREME | | 9 | 11 | 31 | 51 | 0.00% | 0.00% |
| HIGH | 2 | 11 | 10 | 2 | 25 | 44.00% | 9.93% |
| INTERMEDIATE | | 10 | 12 | 3 | 25 | 48.00% | 9.99% |
| LOW | 3 | 19 | 27 | 9 | 58 | 15.52% | 4.75% |
| | 5 | 49 | 60 | 45 | 159 | | |
| Producer's | 0.00% | 22.45% | 20.00% | 20.00% | | 20.13% | 3.18% |
| | 0.00% | 5.96% | 5.16% | 5.96% | | 16.95% | 23.31% |

NI MEAN

| | EXTREME | HIGH | INTERMEDIATE | LOW | | User's | |
|---|---|---|---|---|---|---|---|
| EXTREME | 39 | 11 | 1 | | 51 | 76.47% | 5.94% |
| HIGH | 14 | 6 | 4 | 1 | 25 | 24.00% | 8.54% |
| INTERMEDIATE | | 7 | 3 | 15 | 25 | 12.00% | 6.50% |
| LOW | | 2 | 10 | 46 | 58 | 79.31% | 5.32% |
| | 53 | 26 | 18 | 62 | 159 | | |
| Producer's | 73.58% | 23.08% | 16.67% | 74.19% | | 59.12% | 3.90% |
| | 6.06% | 8.26% | 8.78% | 5.56% | | 55.22% | 63.02% |

NI STDDE

| | EXTREME | HIGH | INTERMEDIATE | LOW | | User's | |
|---|---|---|---|---|---|---|---|
| EXTREME | 33 | 13 | | 5 | 51 | 64.71% | 6.69% |
| HIGH | 14 | 5 | 1 | 5 | 25 | 20.00% | 8.00% |
| INTERMEDIATE | 4 | 7 | 3 | 11 | 25 | 12.00% | 6.50% |
| LOW | 6 | 18 | 6 | 28 | 58 | 48.28% | 6.56% |
| | 57 | 43 | 10 | 49 | 159 | | |
| Producer's | 57.89% | 11.63% | 30.00% | 57.14% | | 43.40% | 3.93% |
| | 6.54% | 4.89% | 14.49% | 7.07% | | 39.47% | 47.33% |

SWI MEAN

| | EXTREME | HIGH | INTERMEDIATE | LOW | | User's | |
|---|---|---|---|---|---|---|---|
| EXTREME | 12 | 6 | 7 | 26 | 51 | 23.53% | 5.94% |
| HIGH | 11 | 6 | 6 | 2 | 25 | 24.00% | 8.54% |
| INTERMEDIATE | 3 | 8 | 14 | | 25 | 56.00% | 9.93% |
| LOW | 4 | 13 | 14 | 27 | 58 | 46.55% | 6.55% |
| | 30 | 33 | 41 | 55 | 159 | | |
| Producer's | 40.00% | 18.18% | 34.15% | 49.09% | | 37.11% | 3.83% |
| | 8.94% | 6.71% | 7.41% | 6.74% | | 33.28% | 40.94% |

SWI STDDE

| | EXTREME | HIGH | INTERMEDIATE | LOW | | User's | |
|---|---|---|---|---|---|---|---|
| EXTREME | 2 | 6 | 12 | 31 | 51 | 3.92% | 2.72% |
| HIGH | 1 | 6 | 14 | 4 | 25 | 24.00% | 8.54% |
| INTERMEDIATE | | 15 | 8 | 2 | 25 | 32.00% | 9.33% |
| LOW | 9 | 34 | 14 | 1 | 58 | 1.72% | 1.71% |
| | 12 | 61 | 48 | 38 | 159 | | |
| Producer's | 16.67% | 9.84% | 16.67% | 2.63% | | 10.69% | 2.45% |
| | 10.76% | 3.81% | 5.38% | 2.60% | | 8.24% | 13.14% |

SWI2 MEAN

| | EXTREME | HIGH | INTERMEDIATE | LOW | | User's | |
|---|---|---|---|---|---|---|---|
| EXTREME | 15 | 18 | 10 | 8 | 51 | 29.41% | 6.38% |
| HIGH | 5 | 9 | 10 | 1 | 25 | 36.00% | 9.60% |
| INTERMEDIATE | | 12 | 13 | | 25 | 52.00% | 9.99% |
| LOW | | 24 | 33 | 1 | 58 | 1.72% | 1.71% |
| | 20 | 63 | 66 | 10 | 159 | | |
| Producer's | 75.00% | 14.29% | 19.70% | 10.00% | | 23.90% | 3.38% |
| | 9.68% | 4.41% | 4.90% | 9.49% | | 20.52% | 27.28% |

SWI2 STDDE

| | EXTREME | HIGH | INTERMEDIATE | LOW | | User's | |
|---|---|---|---|---|---|---|---|
| EXTREME | 16 | 11 | 4 | 20 | 51 | 31.37% | 6.50% |
| HIGH | 4 | 8 | 8 | 5 | 25 | 32.00% | 9.33% |
| INTERMEDIATE | 1 | 5 | 9 | 10 | 25 | 36.00% | 9.60% |
| LOW | 1 | 5 | 13 | 39 | 58 | 67.24% | 6.16% |
| | 22 | 29 | 34 | 74 | 159 | | |
| Producer's | 72.73% | 27.59% | 26.47% | 52.70% | | 45.28% | 3.95% |
| | 9.50% | 8.30% | 7.57% | 5.80% | | 41.34% | 49.23% |

NDVI MEAN

| | EXTREME | HIGH | INTERMEDIATE | LOW | | User's | |
|---|---|---|---|---|---|---|---|
| EXTREME | 38 | 3 | | 10 | 51 | 74.51% | 6.10% |
| HIGH | 21 | 1 | | 3 | 25 | 4.00% | 3.92% |
| INTERMEDIATE | 2 | 9 | 4 | 10 | 25 | 16.00% | 7.33% |
| LOW | | 3 | 4 | 51 | 58 | 87.93% | 4.28% |
| | 61 | 16 | 8 | 74 | 159 | | |
| Producer's | 62.30% | 6.25% | 50.00% | 68.92% | | 59.12% | 3.90% |
| | 6.21% | 6.05% | 17.68% | 5.38% | | 55.22% | 63.02% |

NDVI STDDE

| | EXTREME | HIGH | INTERMEDIATE | LOW | | User's | |
|---|---|---|---|---|---|---|---|
| EXTREME | 27 | 17 | 7 | | 51 | 52.94% | 6.99% |
| HIGH | 10 | 5 | 7 | 3 | 25 | 20.00% | 8.00% |
| INTERMEDIATE | | 1 | 4 | 20 | 25 | 16.00% | 7.33% |
| LOW | | 2 | 11 | 45 | 58 | 77.59% | 5.48% |
| | 37 | 25 | 29 | 68 | 159 | | |
| Producer's | 72.97% | 20.00% | 13.79% | 66.18% | | 50.94% | 3.96% |
| | 7.30% | 8.00% | 6.40% | 5.74% | | 46.98% | 54.91% |

NDBI MEAN

| | EXTREME | HIGH | INTERMEDIATE | LOW | | User's | |
|---|---|---|---|---|---|---|---|
| EXTREME | 4 | 6 | 19 | 22 | 51 | 7.84% | 3.76% |
| HIGH | | 9 | 9 | 7 | 25 | 36.00% | 9.60% |
| INTERMEDIATE | 3 | 11 | 7 | 4 | 25 | 28.00% | 8.98% |
| LOW | 32 | 14 | 5 | 7 | 58 | 12.07% | 4.28% |
| | 39 | 40 | 40 | 40 | 159 | | |
| Producer's | 10.26% | 22.50% | 17.50% | 17.50% | | 16.98% | 2.98% |
| | 4.86% | 6.60% | 6.01% | 6.01% | | 14.00% | 19.96% |

NDBI STDDE

| | EXTREME | HIGH | INTERMEDIATE | LOW | | User's | |
|---|---|---|---|---|---|---|---|
| EXTREME | 23 | 2 | 4 | 22 | 51 | 45.10% | 6.97% |
| HIGH | 14 | 3 | 1 | 7 | 25 | 12.00% | 6.50% |
| INTERMEDIATE | 1 | 7 | 11 | 6 | 25 | 44.00% | 9.93% |
| LOW | 3 | 12 | 19 | 24 | 58 | 41.38% | 6.47% |
| | 41 | 24 | 35 | 59 | 159 | | |
| Producer's | 56.10% | 12.50% | 31.43% | 40.68% | | 38.36% | 3.86% |
| | 7.75% | 6.75% | 7.85% | 6.40% | | 34.51% | 42.22% |

NDBI2 MEAN

| | EXTREME | HIGH | INTERMEDIATE | LOW | | User's | |
|---|---|---|---|---|---|---|---|
| EXTREME | | 2 | 10 | 39 | 51 | 0.00% | 0.00% |
| HIGH | | 4 | 4 | 17 | 25 | 16.00% | 7.33% |
| INTERMEDIATE | 1 | 10 | 7 | 7 | 25 | 28.00% | 8.98% |
| LOW | 16 | 21 | 17 | 4 | 58 | 6.90% | 3.33% |
| | 17 | 37 | 38 | 67 | 159 | | |
| Producer's | 0.00% | 10.81% | 18.42% | 5.97% | | 9.43% | 2.32% |
| | 0.00% | 5.10% | 6.29% | 2.89% | | 7.12% | 11.75% |

NDBI2 STDDE

| | EXTREME | HIGH | INTERMEDIATE | LOW | | User's | |
|---|---|---|---|---|---|---|---|
| EXTREME | 3 | 13 | 23 | 12 | 51 | 5.88% | 3.29% |
| HIGH | 1 | 8 | 12 | 4 | 25 | 32.00% | 9.33% |
| INTERMEDIATE | 1 | 1 | 13 | 10 | 25 | 52.00% | 9.99% |
| LOW | | 5 | 35 | 18 | 58 | 31.03% | 6.07% |
| | 5 | 27 | 83 | 44 | 159 | | |
| Producer's | 60.00% | 29.63% | 15.66% | 40.91% | | 26.42% | 3.50% |
| | 21.91% | 8.79% | 3.99% | 7.41% | | 22.92% | 29.91% |

NDWI MEAN

| | EXTREME | HIGH | INTERMEDIATE | LOW | | User's | |
|---|---|---|---|---|---|---|---|
| EXTREME | 32 | 9 | | 10 | 51 | 62.75% | 6.77% |
| HIGH | 14 | 11 | | | 25 | 44.00% | 9.93% |
| INTERMEDIATE | | 9 | 7 | 9 | 25 | 28.00% | 8.98% |
| LOW | | 3 | 6 | 49 | 58 | 84.48% | 4.75% |
| | 46 | 32 | 13 | 68 | 159 | | |
| Producer's | 69.57% | 34.38% | 53.85% | 72.06% | | 62.26% | 3.84% |
| | 6.78% | 8.40% | 13.83% | 5.44% | | 58.42% | 66.11% |

NDWI STDDE

| | EXTREME | HIGH | INTERMEDIATE | LOW | | User's | |
|---|---|---|---|---|---|---|---|
| EXTREME | 28 | 17 | 1 | 5 | 51 | 54.90% | 6.97% |
| HIGH | 12 | 6 | 1 | 6 | 25 | 24.00% | 8.54% |
| INTERMEDIATE | 1 | 4 | 6 | 14 | 25 | 24.00% | 8.54% |
| LOW | 3 | 15 | 15 | 25 | 58 | 43.10% | 6.50% |
| | 44 | 42 | 23 | 50 | 159 | | |
| Producer's | 63.64% | 14.29% | 26.09% | 50.00% | | 40.88% | 3.90% |
| | 7.25% | 5.40% | 9.16% | 7.07% | | 36.98% | 44.78% |

ALL MEAN

| | EXTREME | HIGH | INTERMEDIATE | LOW | | User's | |
|---|---|---|---|---|---|---|---|
| EXTREME | 13 | 9 | 14 | 15 | 51 | 25.49% | 6.10% |
| HIGH | 16 | 5 | 4 | | 25 | 20.00% | 8.00% |
| INTERMEDIATE | 5 | 18 | 2 | | 25 | 8.00% | 5.43% |
| LOW | 4 | 22 | 20 | 12 | 58 | 20.69% | 5.32% |
| | 38 | 54 | 40 | 27 | 159 | | |
| Producer's | 34.21% | 9.26% | 5.00% | 44.44% | | 20.13% | 3.18% |
| | 7.70% | 3.94% | 3.45% | 9.56% | | 16.95% | 23.31% |

ALL STDDE

| | EXTREME | HIGH | INTERMEDIATE | LOW | | User's | |
|---|---|---|---|---|---|---|---|
| EXTREME | 1 | 4 | 11 | 35 | 51 | 1.96% | 1.94% |
| HIGH | 1 | 2 | 15 | 7 | 25 | 8.00% | 5.43% |
| INTERMEDIATE | | 12 | 10 | 3 | 25 | 40.00% | 9.80% |
| LOW | 1 | 33 | 17 | 7 | 58 | 12.07% | 4.28% |
| | 3 | 51 | 53 | 52 | 159 | | |
| Producer's | 33.33% | 3.92% | 18.87% | 13.46% | | 12.58% | 2.63% |
| | 27.22% | 2.72% | 5.37% | 4.73% | | 9.95% | 15.21% |

## 8.2 APPENDIX 2 – Python Code For Merge to Biggest Adjacent

```
iteration = 0
shape = ".shp"
filename = ""
name = "area_from_street"
count = 0


while  True :
     iteration+=1
     filename = str(iteration)+shape
     arcpy.SelectLayerByAttribute_management(name,"NEW_SELECTION",'"AREA"<=150000')
     count = int(arcpy.GetCount_management(name).getOutput(0))
     arcpy.Eliminate_management(name,filename)
     name = iteration
     arcpy.CalculateField_management(name, "AREA","!Shape_Area!", "PYTHON_9.3")
     print count
     if count < 1:
         break

2760
536
62
1
0
```